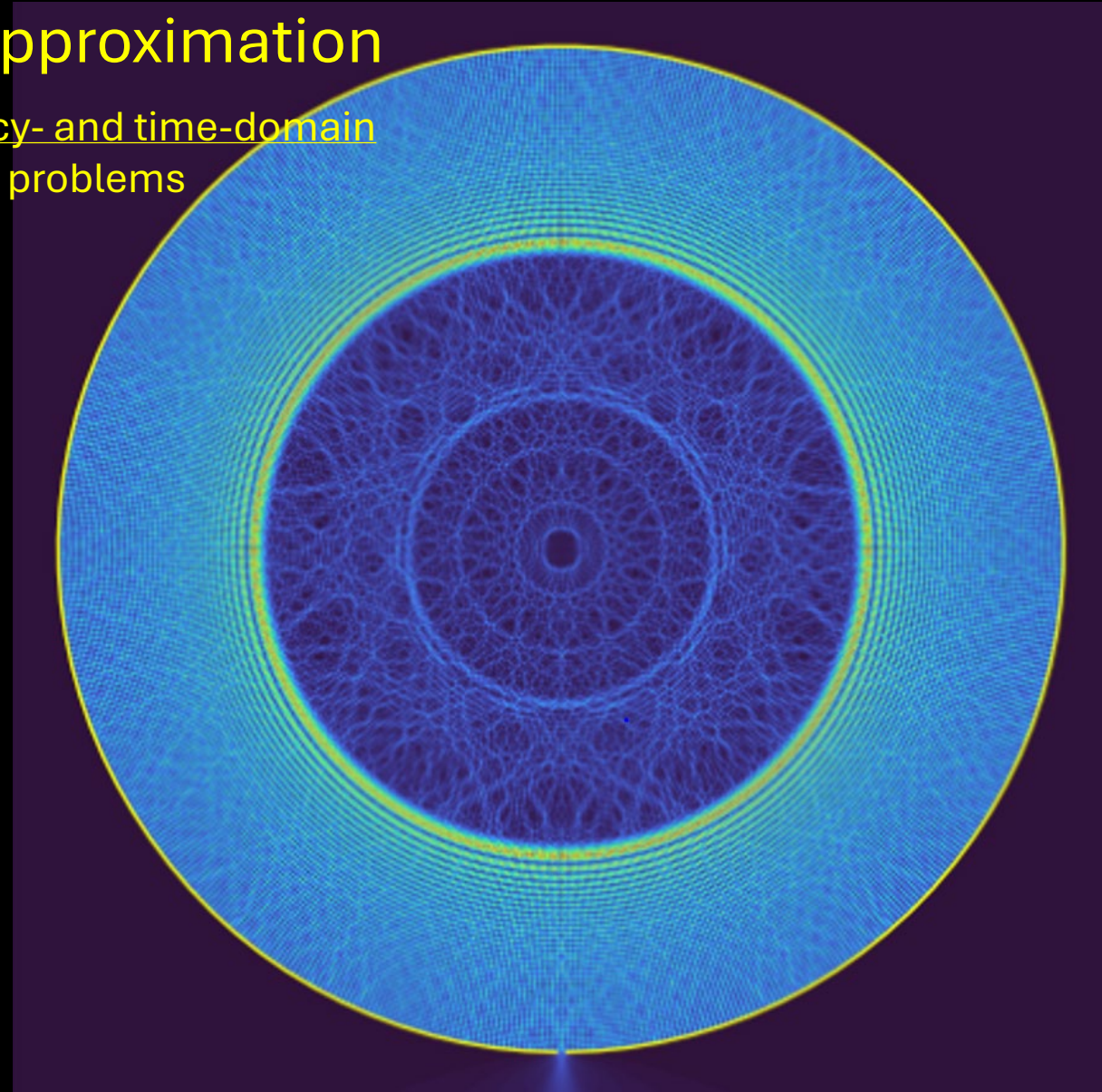
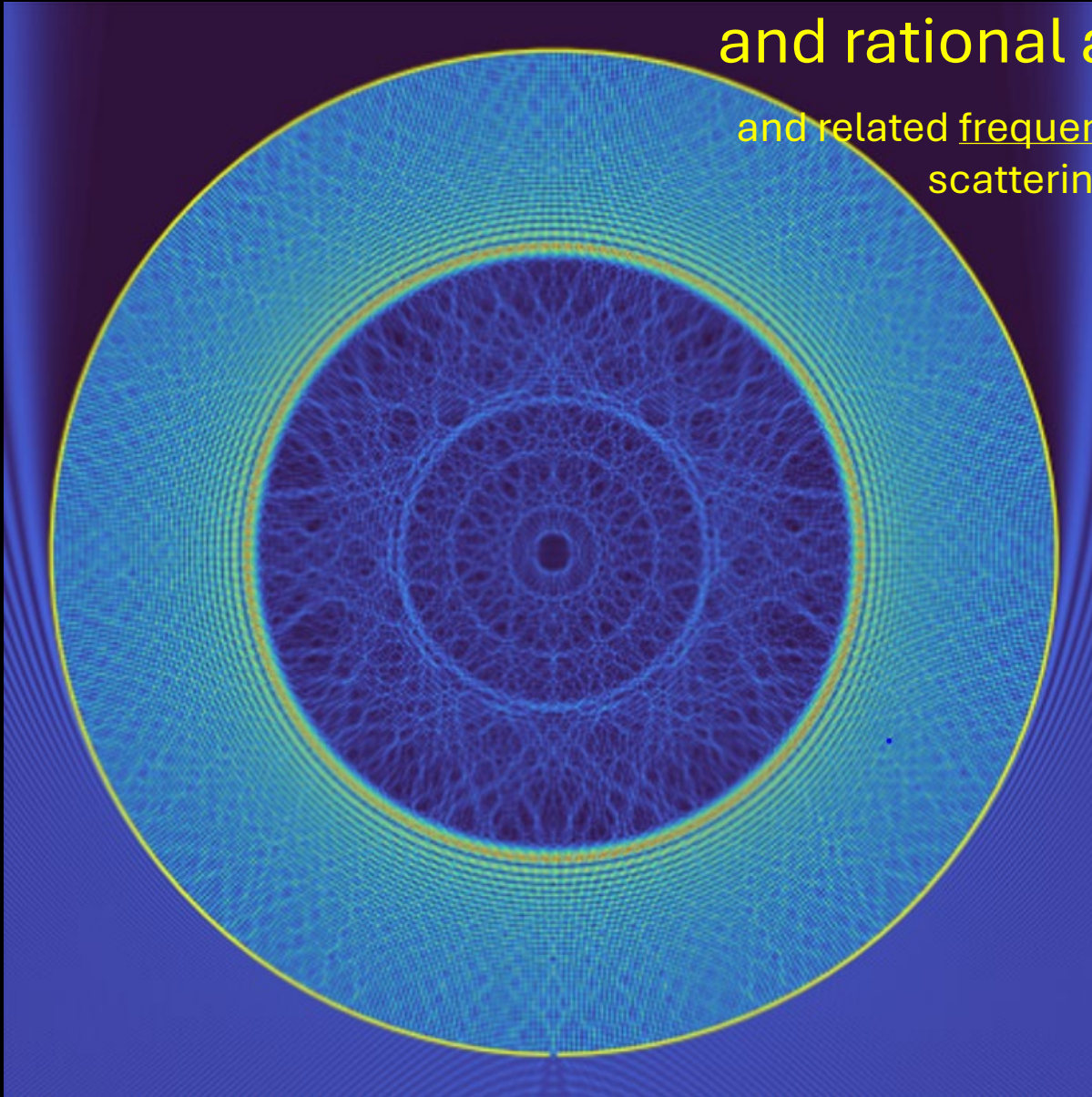
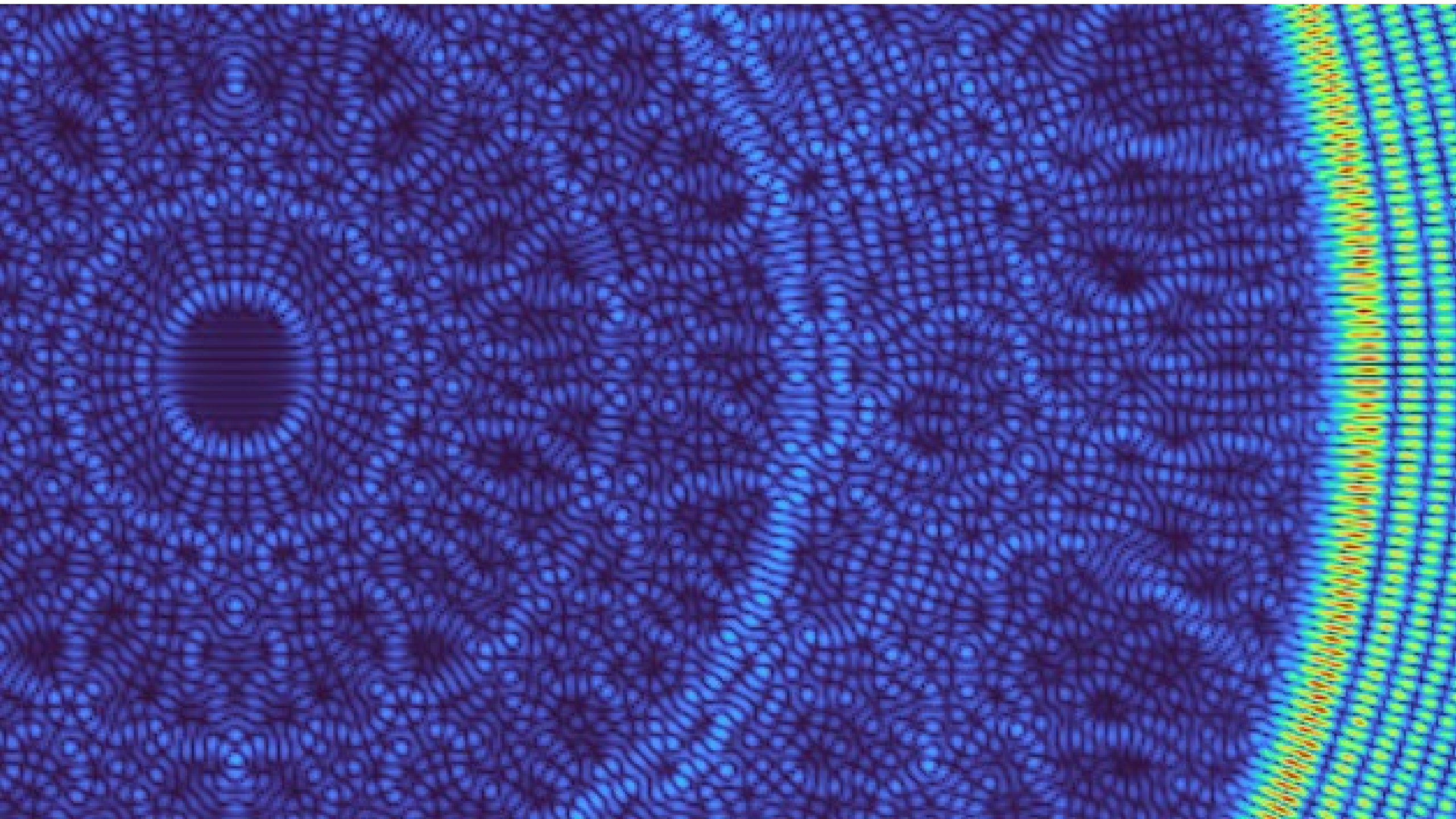


# Evaluation of resonances via adaptivity and rational approximation

and related frequency- and time-domain  
scattering problems

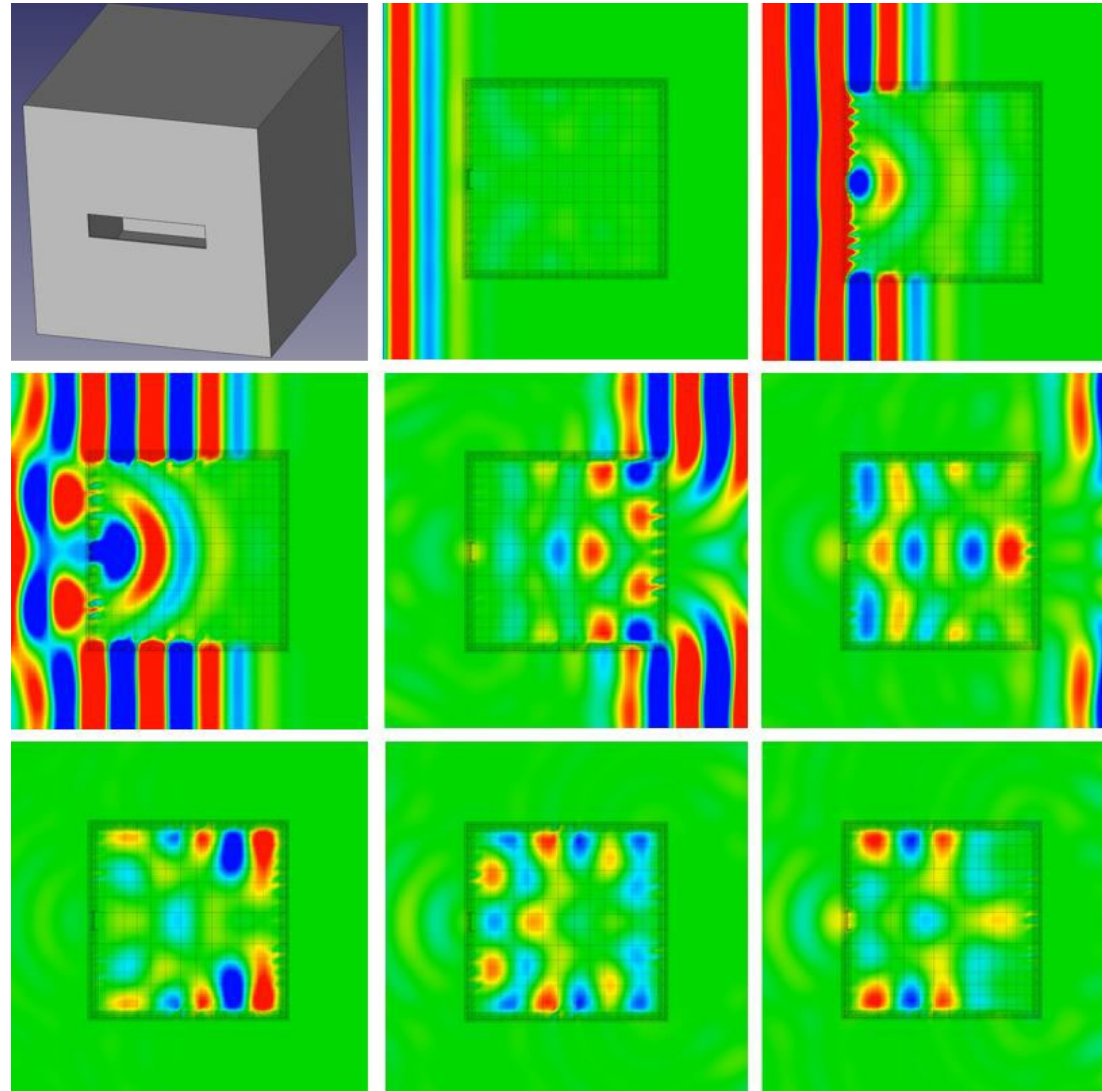






But...

## Open Cavity Problems



Frequency-Time Hybrid (FTH) time-domain algorithm: an effective time-domain wave solver

Open Cavity problems: Accumulation of slowly decaying cycles over multiple incidence windows (expensive)

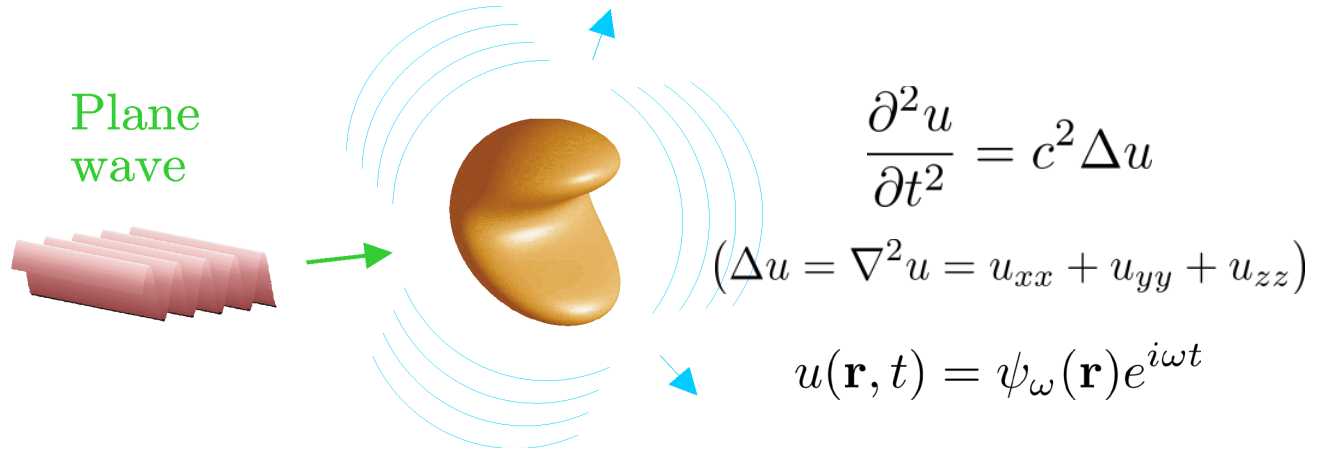
Open Cavity problems: Require many frequency-domain solutions (expensive)

Resonant

# Pure Frequencies

(Time Harmonic Waves)

$$\nabla \times \mathbf{H} = \mathbf{J} + \frac{\partial \mathbf{D}}{\partial t}$$
$$\nabla \times \mathbf{E} + \frac{\partial \mathbf{B}}{\partial t} = 0$$



Electromagnetic

$$\nabla \times \mathbf{E} = i\omega\mu\mathbf{H}$$

$$\nabla \times \mathbf{H} = -i\omega\epsilon\mathbf{E}$$

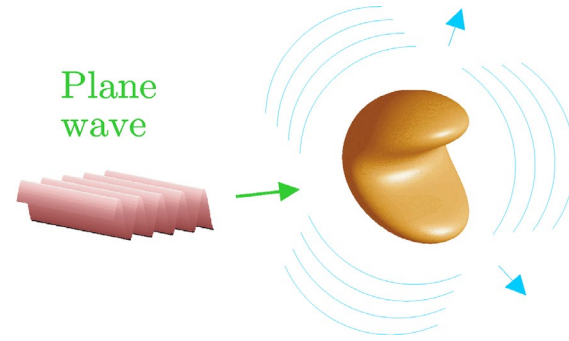
Acoustic

$$\Delta\psi(\mathbf{r}) + k^2\psi(\mathbf{r}) = 0$$



# Simple integral equation example

$$\Delta\psi^{\text{scatt}}(\mathbf{r}) + k^2\psi^{\text{scatt}}(\mathbf{r}) = 0$$



$$\psi^{\text{scatt}}(\mathbf{r}) = \int_S G_k(\mathbf{r}, \mathbf{r}') \mu(\mathbf{r}') dS'$$

$$\int_S G_k(\mathbf{r}, \mathbf{r}') \mu(\mathbf{r}') dS' = -\psi^{\text{inc}}(\mathbf{r}) \quad \mathbf{r} \in S$$

$$G_k(\mathbf{r}, \mathbf{r}') = \begin{cases} H_0^1(k|\mathbf{r} - \mathbf{r}'|) & \text{in two dimensions} \\ e^{ik|\mathbf{r} - \mathbf{r}'|}/|\mathbf{r} - \mathbf{r}'| & \text{in three dimensions} \end{cases}$$

Iterative linear algebra solution...

# Well-posed Electromagnetic Integral Equation Formulation

## CFIE-R

$$\frac{\mathbf{J}}{2} + \mathcal{K}\mathbf{J} + \xi k (\mathbf{n} \times \mathcal{R}) \circ \mathcal{T}\mathbf{J} = \mathbf{n} \times \mathbf{H}^i - \xi k (\mathbf{n} \times \mathcal{R})(\mathbf{n} \times \mathbf{E}^i)$$

$$\mathcal{K}\vec{\mathbf{J}}(\mathbf{x}) = \mathbf{n}(\mathbf{x}) \times \int_{\Gamma} \nabla_{\mathbf{x}'} G_k(\mathbf{x}, \mathbf{x}') \times \vec{\mathbf{J}}(\mathbf{x}') d\sigma(\mathbf{x}') \quad \mathcal{T}\vec{\mathbf{J}}(\mathbf{x}) = k^2 \int_{\Gamma} G_k(\mathbf{x}, \mathbf{x}') \vec{\mathbf{J}}(\mathbf{x}') d\sigma(\mathbf{x}') + \int_{\Gamma} \nabla_{\mathbf{x}'} G_k(\mathbf{x}, \mathbf{x}') \operatorname{div}_{\Gamma} \vec{\mathbf{J}}(\mathbf{x}') d\sigma(\mathbf{x}') \quad S\psi(\mathbf{x}) = \int_{\Gamma} G_k(\mathbf{x} - \mathbf{x}') \psi(\mathbf{x}') d\sigma(\mathbf{x}')$$

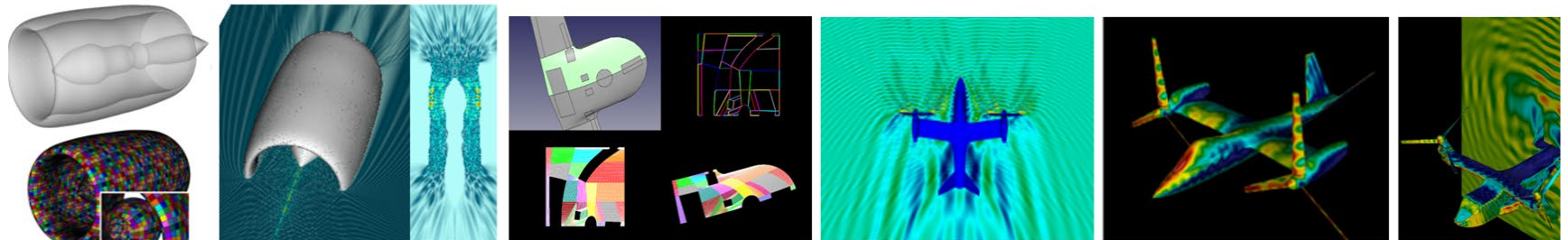
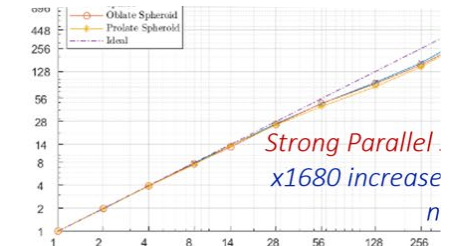
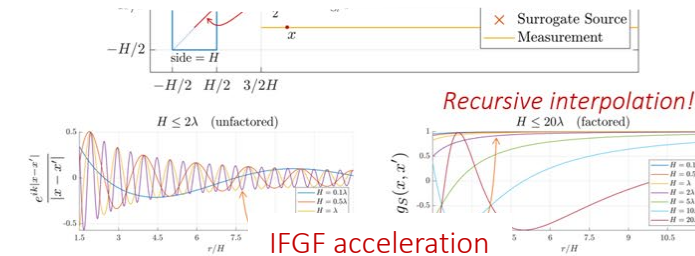
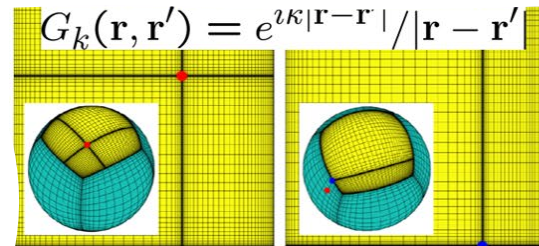
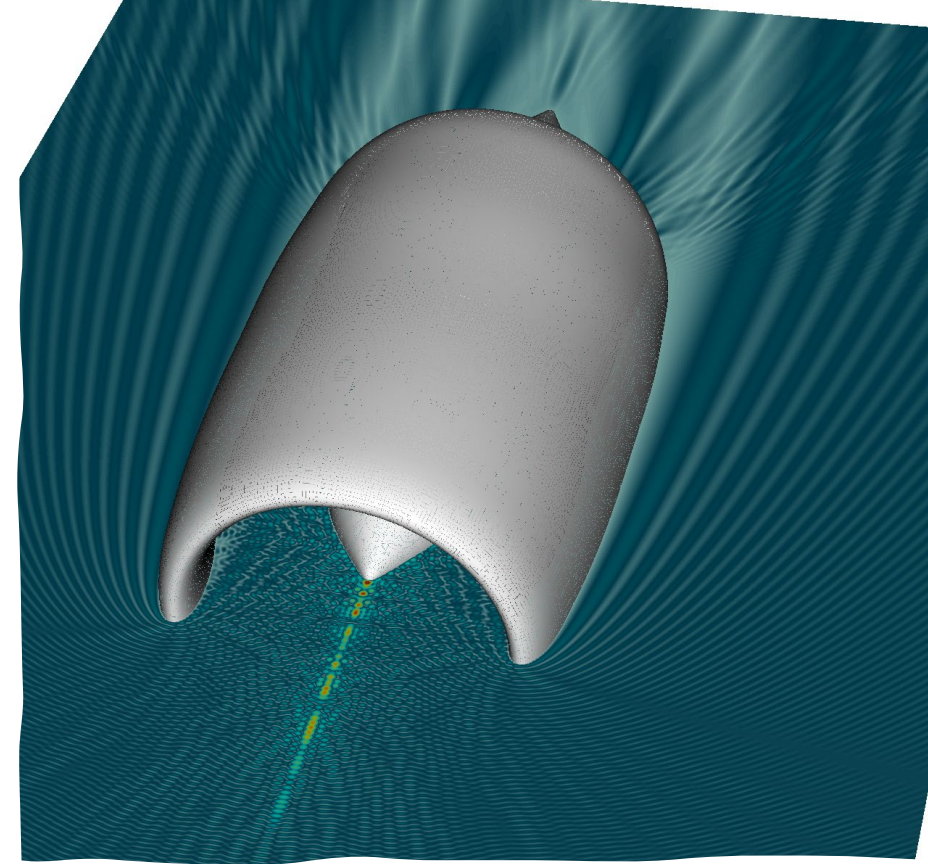
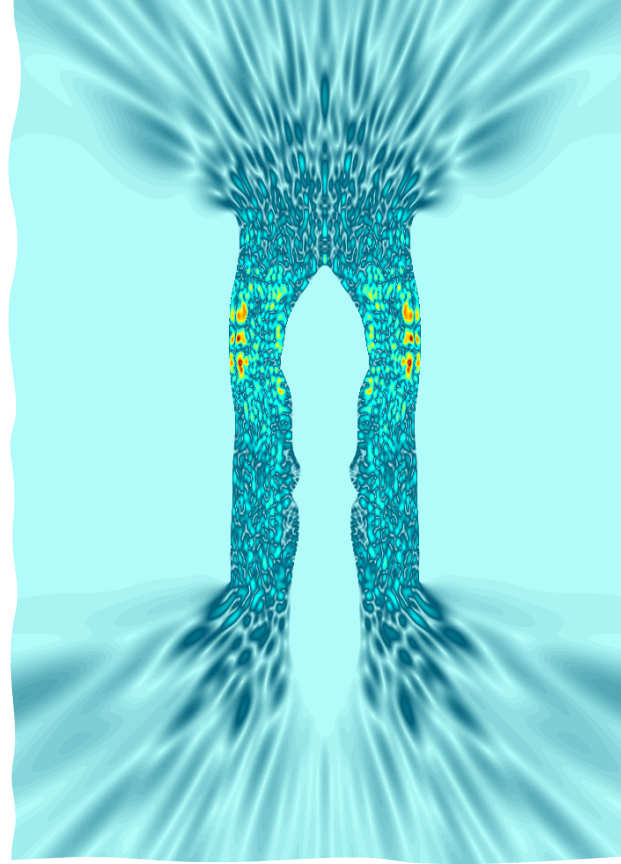
Theorem (General surface, arbitrary wavenumber  $k$ ):

Using  $\mathcal{R} = S_K$ ,  $K = ik/2$  we have  $\left( S_K \psi(\mathbf{x}) = \int_{\Gamma} G_K(\mathbf{x} - \mathbf{x}') \psi(\mathbf{x}') d\sigma(\mathbf{x}') \right)$

- CFIE-R are uniquely solvable;
- CFIE-R  $\leftrightarrow$  Invertible diagonal operator + Compact operator
- Small iteration numbers

Bruno, Elling, Paffenroth and Turc, J. Comput. Phys. [2009]

# Versatile, accurate, efficient





Frequency-Time hybrids

# “Hybrid” Time-domain from frequency domain

Time-parallel, time-leaping, wave equation/Maxwell solver

$$\frac{\partial^2 u}{\partial t^2} = c^2 \Delta u$$

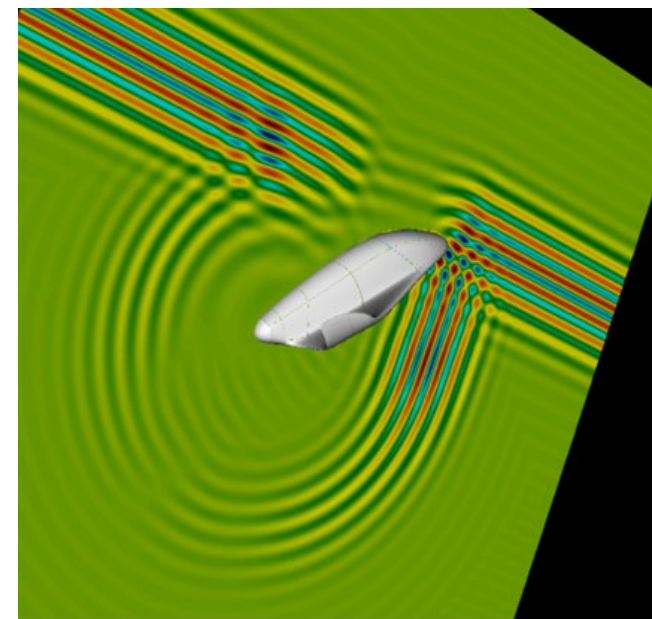
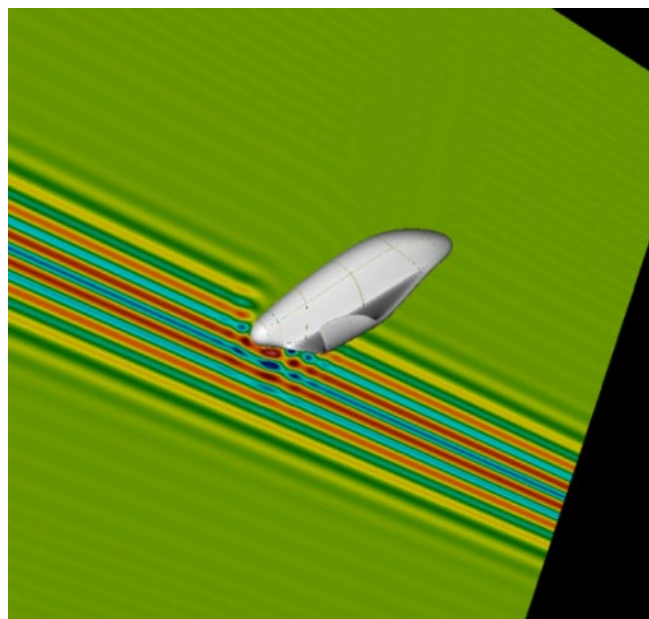
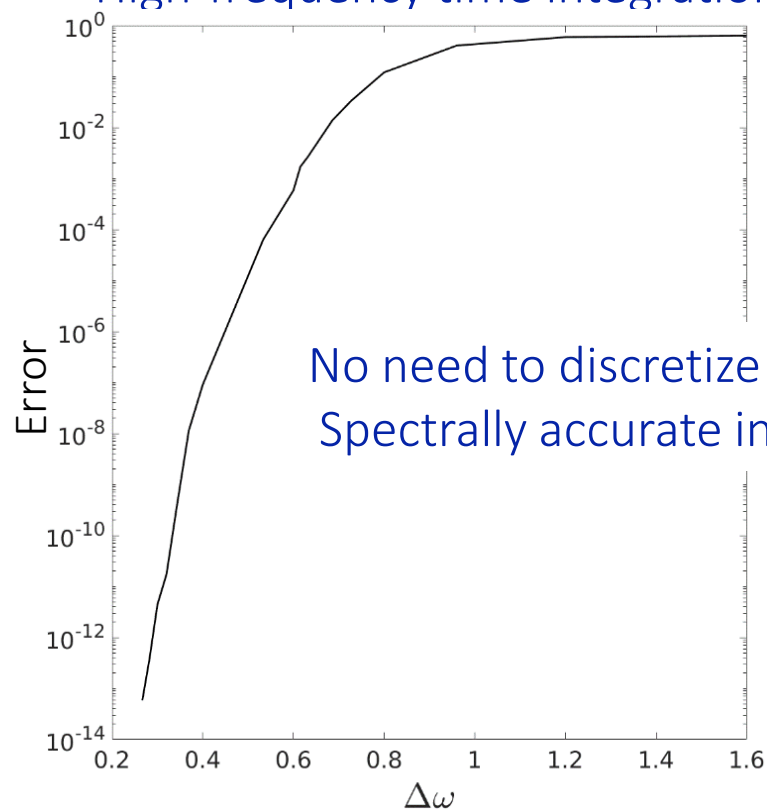
Freq. Domain vs. Time Transients:

$\longleftrightarrow$   
(Fourier Transform)

$$\Delta \psi_\omega + k^2 \psi_\omega = 0, \quad k = \frac{\omega}{c}$$

$$u(\mathbf{r}, t) = \int_{-\infty}^{\infty} \psi_\omega(\mathbf{r}) e^{i\omega t} d\omega$$

Windowing and recentering  
High-frequency time integration



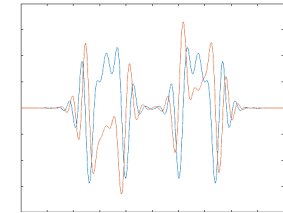
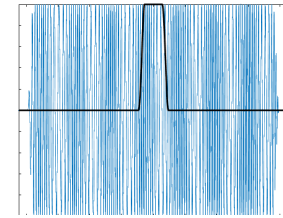
# Smooth Incident-Field Time Partitioning



- Use a partition of unity to decompose the long duration signal  $u^{inc}(x, t)$  into multiple relatively short duration signals which require only a fixed discretization in frequency space.

$$F_k(\omega) = \int_{-T}^T w_k(t) u^{inc}(x, t) e^{i\omega t} dt = \int_{t_k-h}^{t_k+h} w_k(t) u^{inc}(x, t) e^{i\omega t} dt$$

$$= \boxed{e^{i\omega t_k}} \int_{-h}^h w_k(t + t_k) u^{inc}(x, t + t_k) e^{i\omega t} dt$$



- Using the same discretization in frequency space for each time-windowed problem, the Helmholtz solutions at each frequency may be reused.

$$\int_{-h}^h w_k(t + t_k) u^{inc}(x, t + t_k) e^{i\omega t} dt \longrightarrow \hat{G}_k(x, \omega)$$



# Time evolution via FFT-based “scaled convolution”

After time windowing and recentering,  $u^{inc}(x, \omega)$ , and thus, the solution  $u(x, \omega)$ , become a slowly varying, approximately band-limited functions of  $\omega$ :

$$u(x, t) = \int_{-\infty}^{\infty} u(x, \omega) e^{-i\omega t} d\omega \approx \int_{-W}^W u(x, \omega) e^{-i\omega t} d\omega$$

Higher frequency integration for larger  $t$ ! Substitute  $u(x, \omega)$  by its truncated Fourier Series approximation in  $\omega$ :

$$u(x, t) \approx \sum_{m=-N/2}^{N/2-1} c_m(x) \int_{-W}^W e^{i\frac{\pi}{W}(m-\frac{W}{\pi}t)\omega} d\omega = \sum_{m=-N/2}^{N/2-1} c_m(x) (2W \text{sinc}(\alpha t - m))$$

Then, discretizing in  $t$  we obtain a “scaled convolution”:

$$u(x, t_\ell) \approx \sum_{m=-N/2}^{N/2-1} c_m b_{\beta\ell-m}, \quad \text{where} \quad b_q = 2W \text{sinc}(q)$$

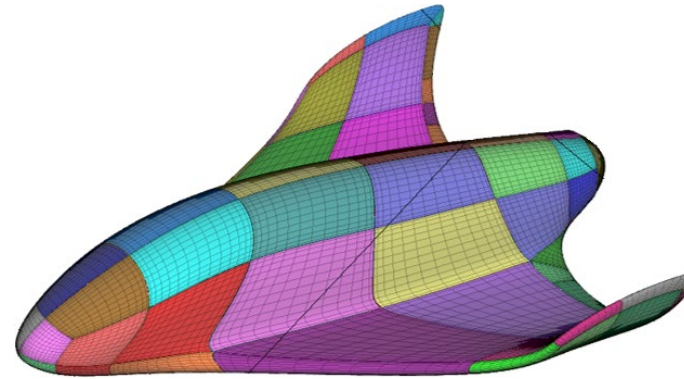
Use FFT-accelerated *Fractional Fourier Transform*-based  
scaled discrete convolutions

# Benefits

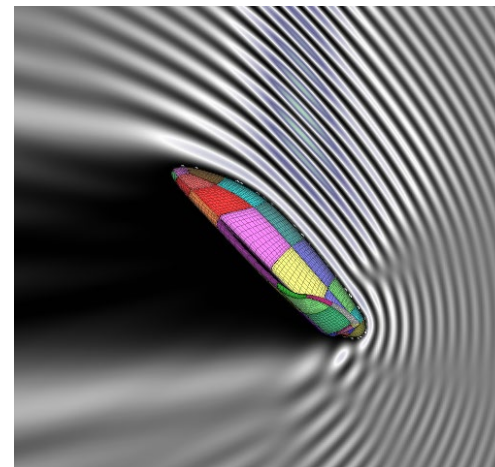
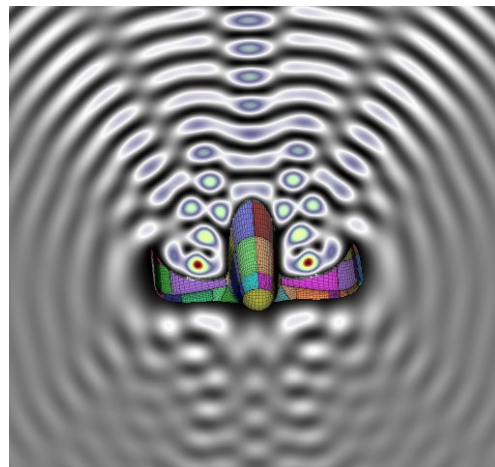
- Overall cost: linear in time and proportional to the cost of the frequency domain solver. Less expensive asymptotics than FDTD.
- No time-domain numerical dispersion error (!!).
- Natural Parallelism for frequency-domain solutions.
- Natural Parallelism in time! (cf. P. L. Lions “para-real” algorithm).
- Time- and Space-Leaping (!!).
- $O(1)$  cost for solution sampling at arbitrarily large times (!!)
- Use of absorbing boundaries, PML, etc., not necessary.
- High-order accuracy (fast/accurate high-frequency integration).

# Example: High-altitude glider

## NASA's X-24A Lifting Body



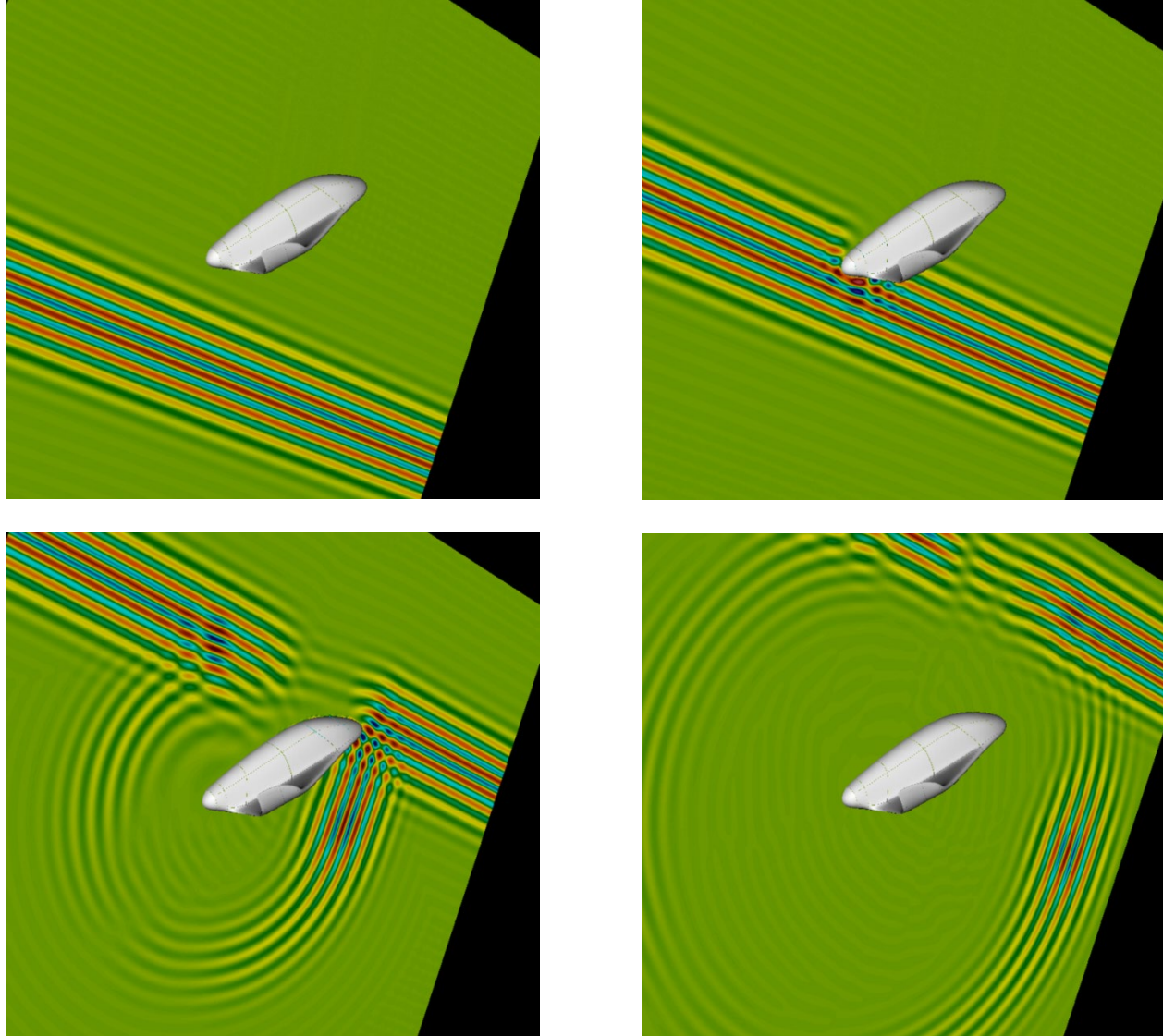
Utilizing frequency-domain solutions...



(Bruno and Garza, "Rectangular-polar integral solver", arXiv [2018])



...the Fast-Hybrid method produces solutions in the time domain



Anderson, Bruno and Lyon [2018]

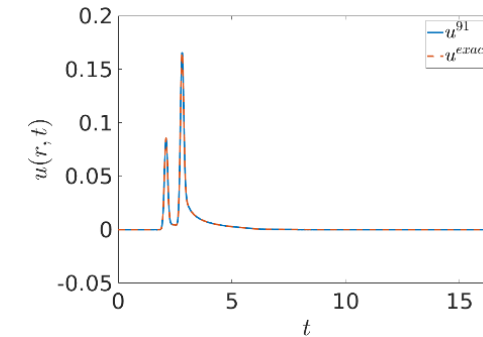
# Cost comparisons\*\* with...

...time-domain integral equations *and* convolution quadrature

Significant advantages even for short (Gaussian) incident pulses

(worst case for hybrid method)

—	$\ e\ _\infty$	CPU Time (hrs)	Mem (GB)
Hybrid method (unaccel.)	$2.2 \cdot 10^{-4}$	4.3	1.6
[BK14] (accel.)	$2.1 \cdot 10^{-3}$	40.1	56.8



—	$\ e\ _\infty$	Wall Time (mins)	Mem (GB)
Hybrid method (unaccel.)	$1.6 \cdot 10^{-7}$	4.1	1.2
[BGH19] (unaccel.)	$\approx 10^{-7}$	101.75	290

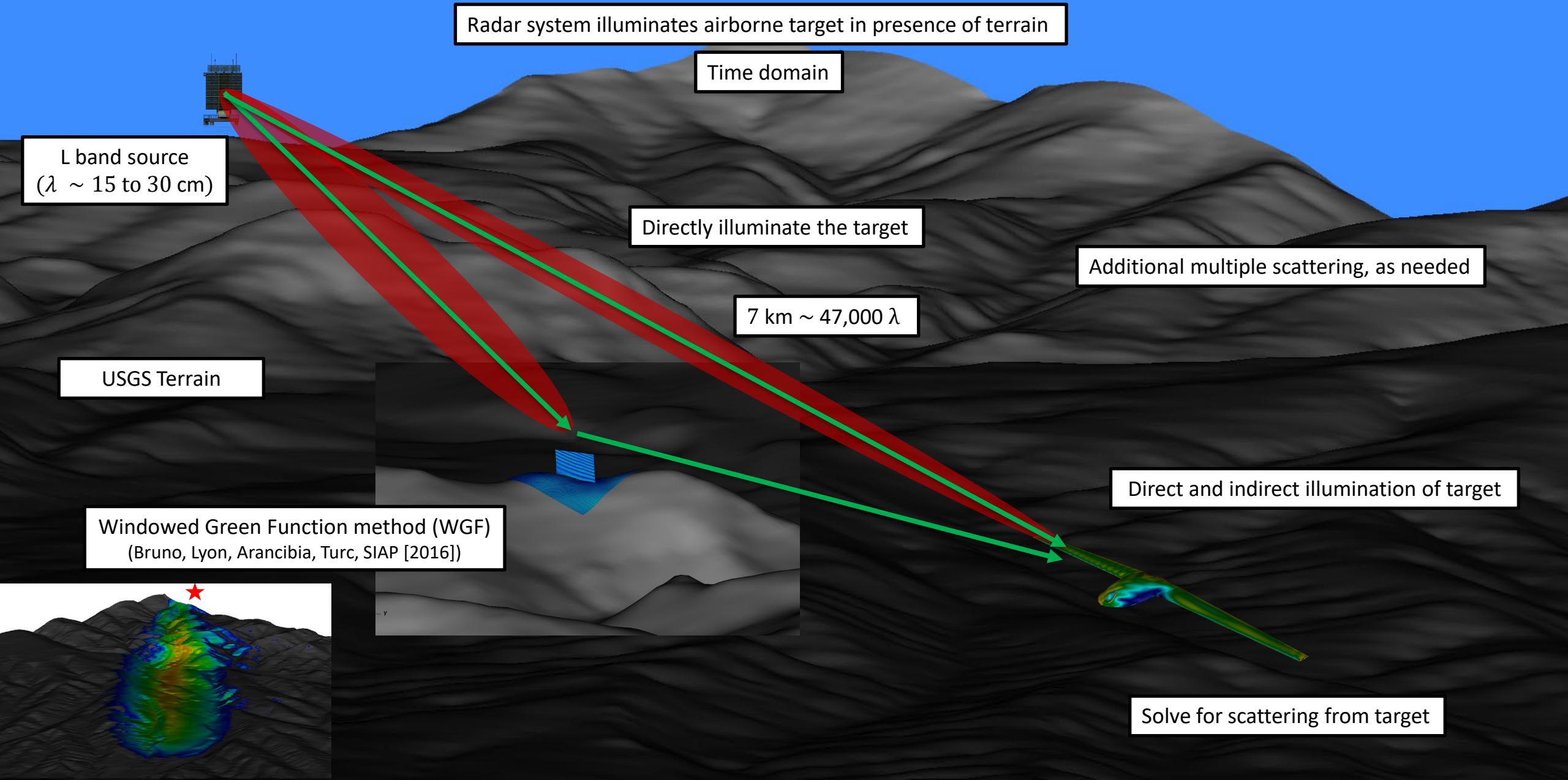
[BK14]: L. Banjai and M. Kachanovska, *Fast convolution quadrature for the wave equation in three dimensions*, JCP, (2014)

[BGH19]: A. H. Barnett, L. Greengard, and T. Hagstrom, *High-order discretization of a stable time-domain integral equation for 3d acoustic scattering*, JCP, (2020)

\*\*For full details concerning these comparisons see the arXiv publication

[ABL20] T. G. Anderson, O. P. Bruno and M. Lyon, *High-order, Dispersionless "Fast-Hybrid" Wave Equation Solver. Part I:  $O(1)$  Sampling Cost via Incident-Field Windowing and Recentering*, SISC, (2020)

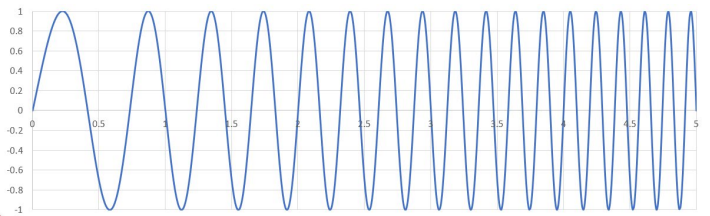
# Time-domain scattering in presence of terrain



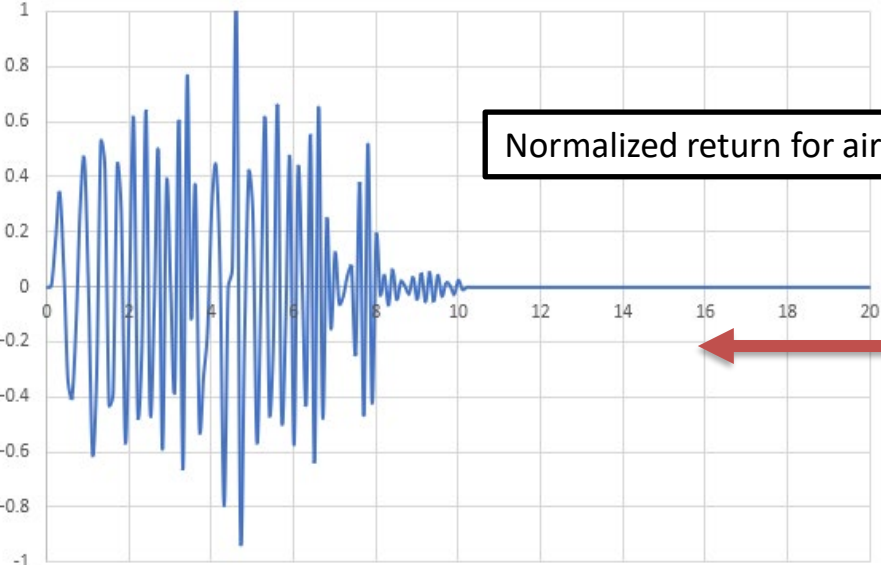


Combine Frequency Domain solutions to recover Time Domain

Original Signal - Linear chirp waveform

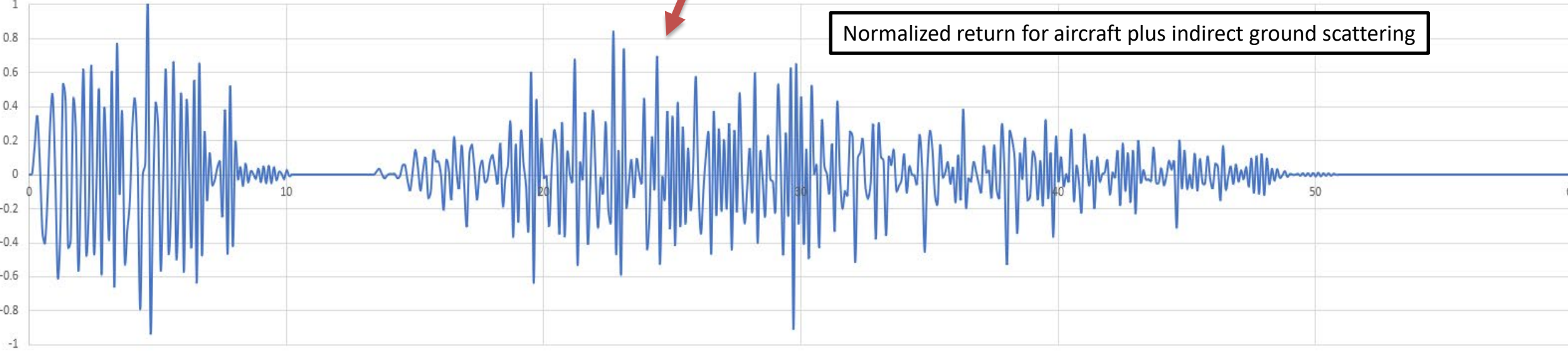


Normalized return for aircraft alone



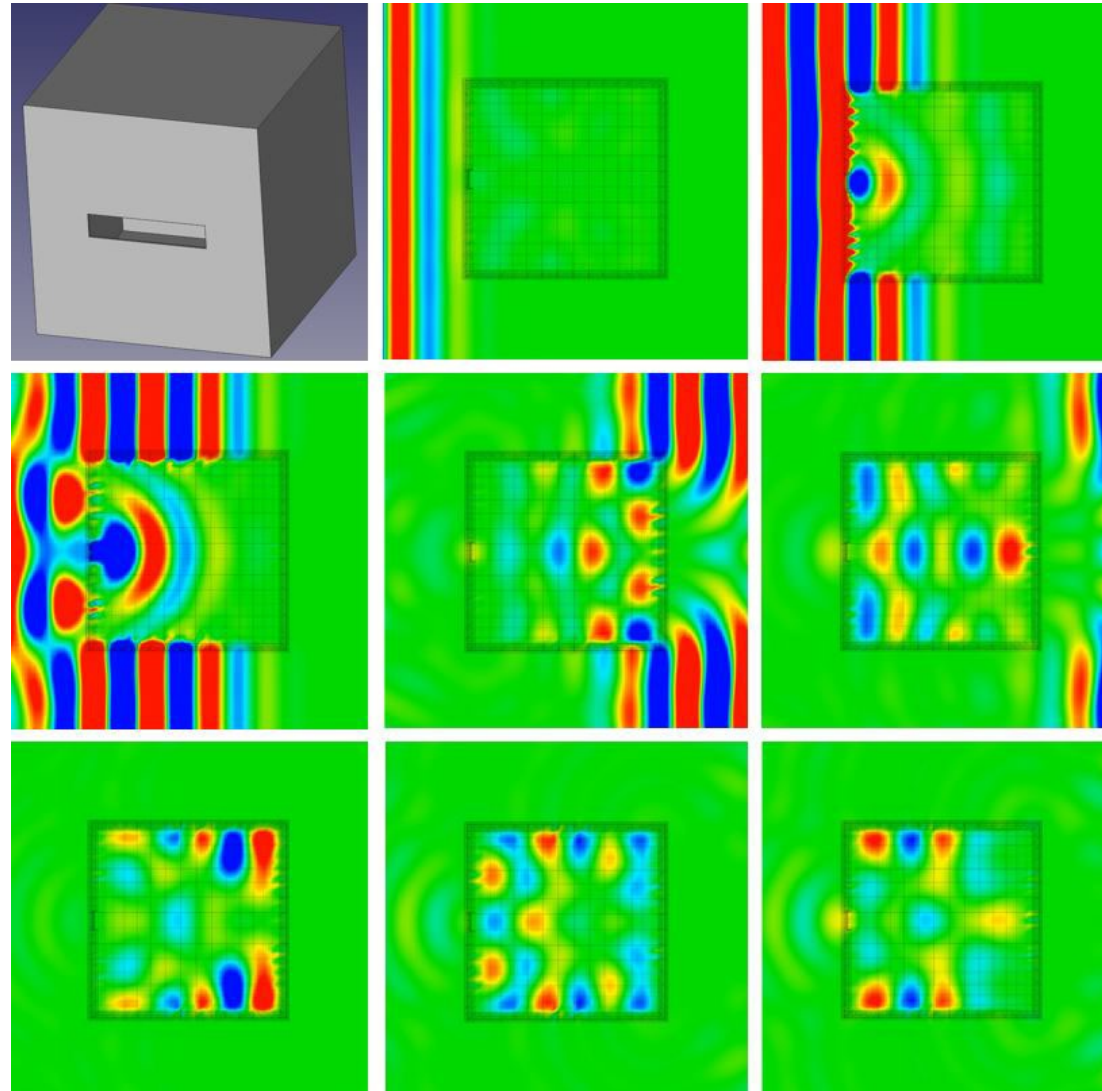
Time Domain Solver

Normalized return for aircraft plus indirect ground scattering



But...

## Open Cavity Problems



Resonant

Frequency-Time Hybrid (FTH) time-domain algorithm: an effective time-domain wave solver

Open Cavity problems: Accumulation of slowly decaying cycles over multiple incidence windows (expensive)

Open Cavity problems: Require many frequency-domain solutions (expensive)

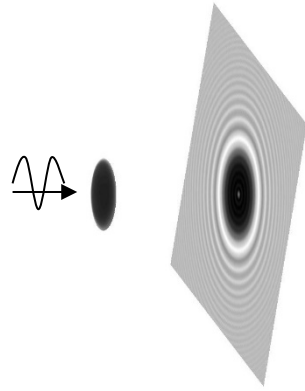


# Open Surface Problems (Helmholtz and Maxwell equations)

Dirichlet Problem

$$\Delta u + k^2 u = 0$$

$$u|_{\Gamma} = f$$



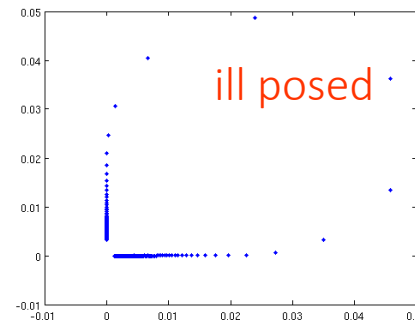
Neumann Problem

$$\Delta v + k^2 v = 0$$

$$\partial v / \partial n|_{\Gamma} = g$$

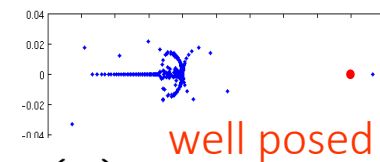
$$S(\varphi)(x) = \int_{\Gamma} G(x, y) \varphi(y) dS_y = f(x)$$

$$N(\psi)(x) = \int_{\Gamma} \frac{\partial^2}{\partial n_x \partial n_y} G(x, y) \psi(y) dS_y = g(x)$$



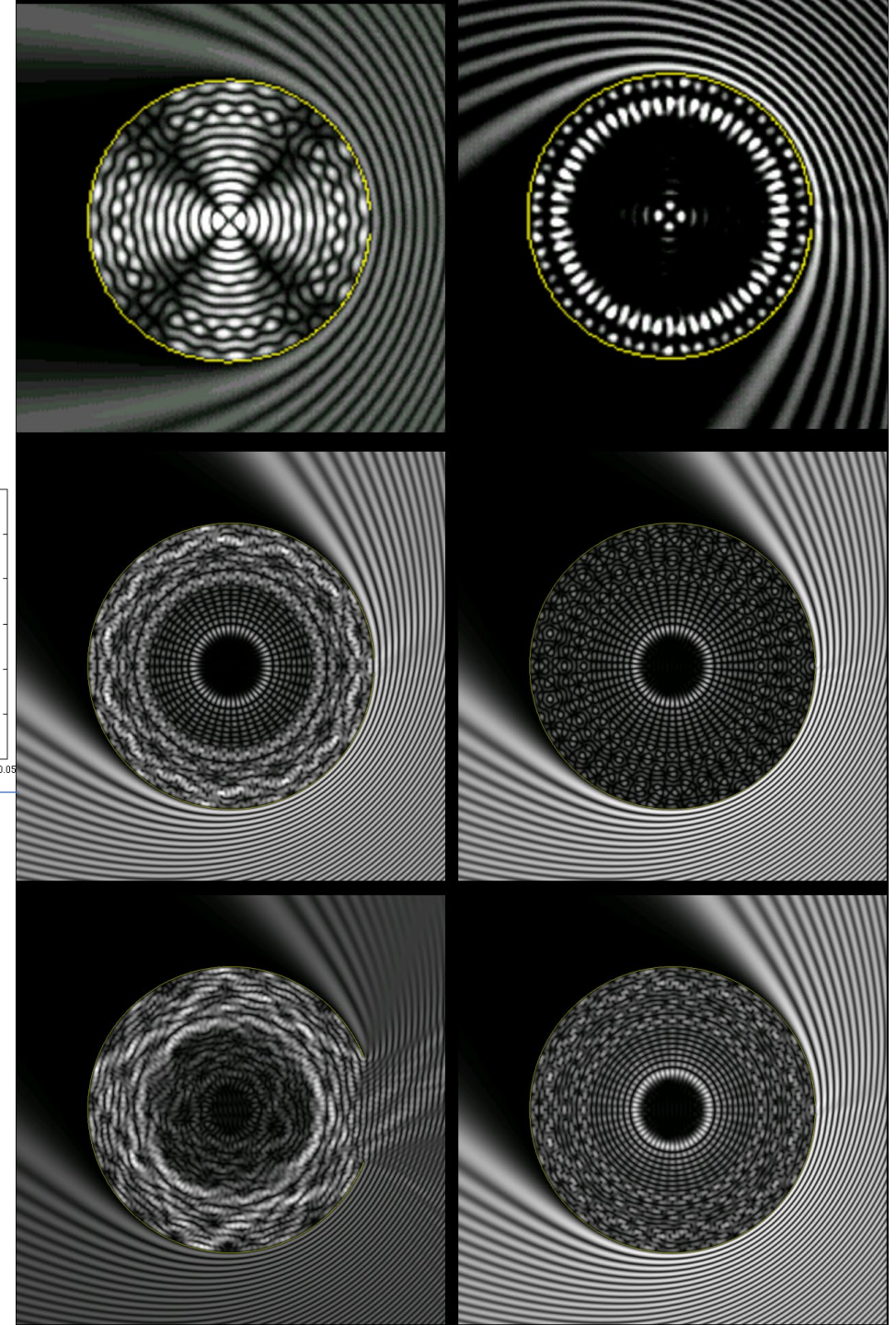
$$S_{\omega}(\varphi)(x) = \int_{\Gamma} G(x, y) \frac{\varphi(y)}{\omega(y)} dS_y$$

$$N_{\omega}(\psi)(x) = \int_{\Gamma} \frac{\partial^2}{\partial n_x \partial n_y} G(x, y) \psi(y) \omega(y) dS_y = g(x)$$

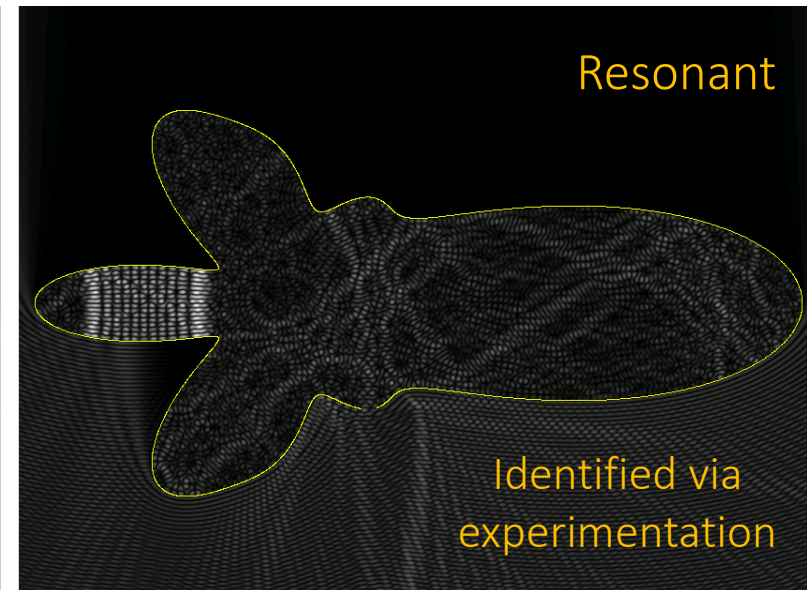
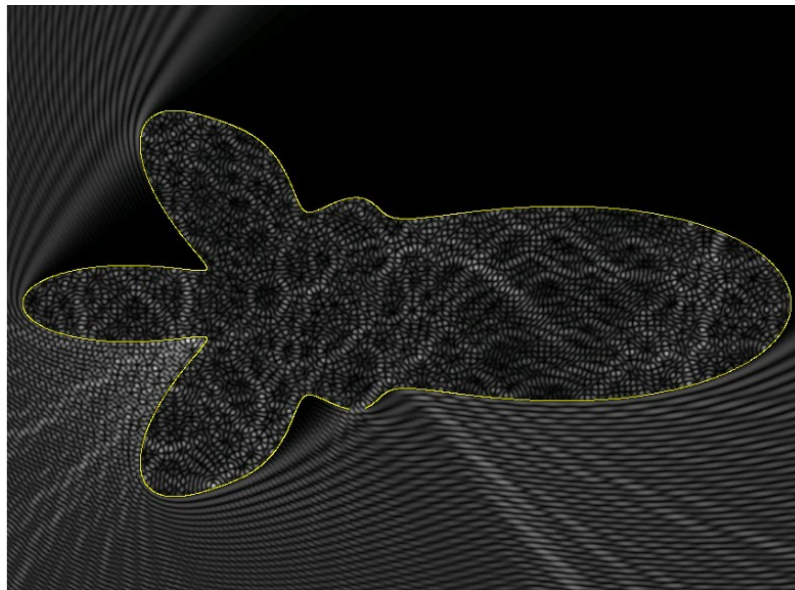
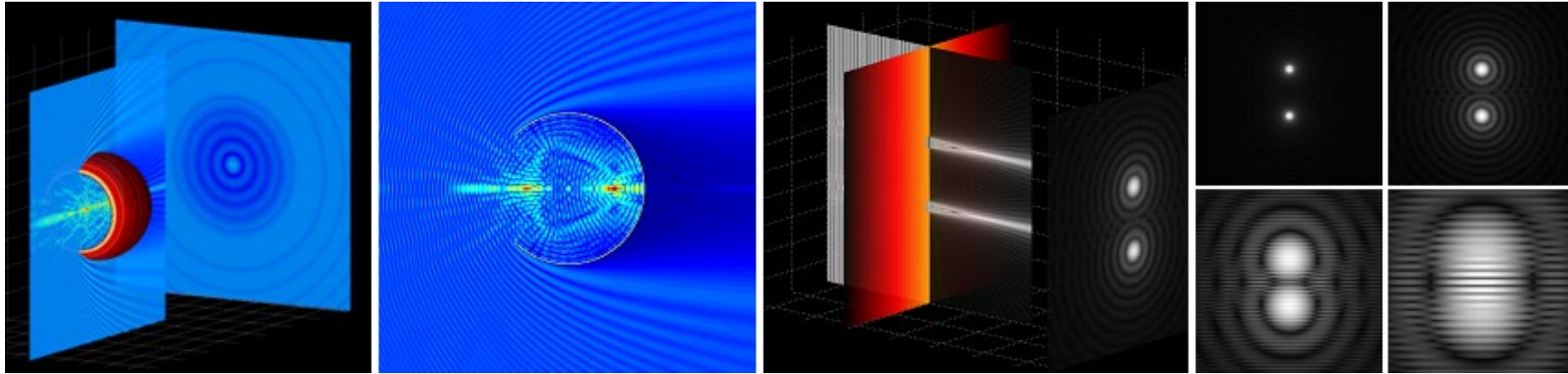


$$N_{\omega} S_{\omega}(\varphi) = -\frac{\varphi}{4} + \int_{\Gamma} \varphi(z) K_{\omega}(x, z) dz \quad \text{where} \quad K_{\omega}(x, z) \sim \frac{1}{|x-z|}$$

Bruno and Lintner [2012, 2015]: Calderón formula; Second-kind formulation for open surfaces; Cesaro operator (cf. Povzner-Sukharevskii [1960]).



# 3D Open Surface Problems, incl. open cavities (frequency domain)

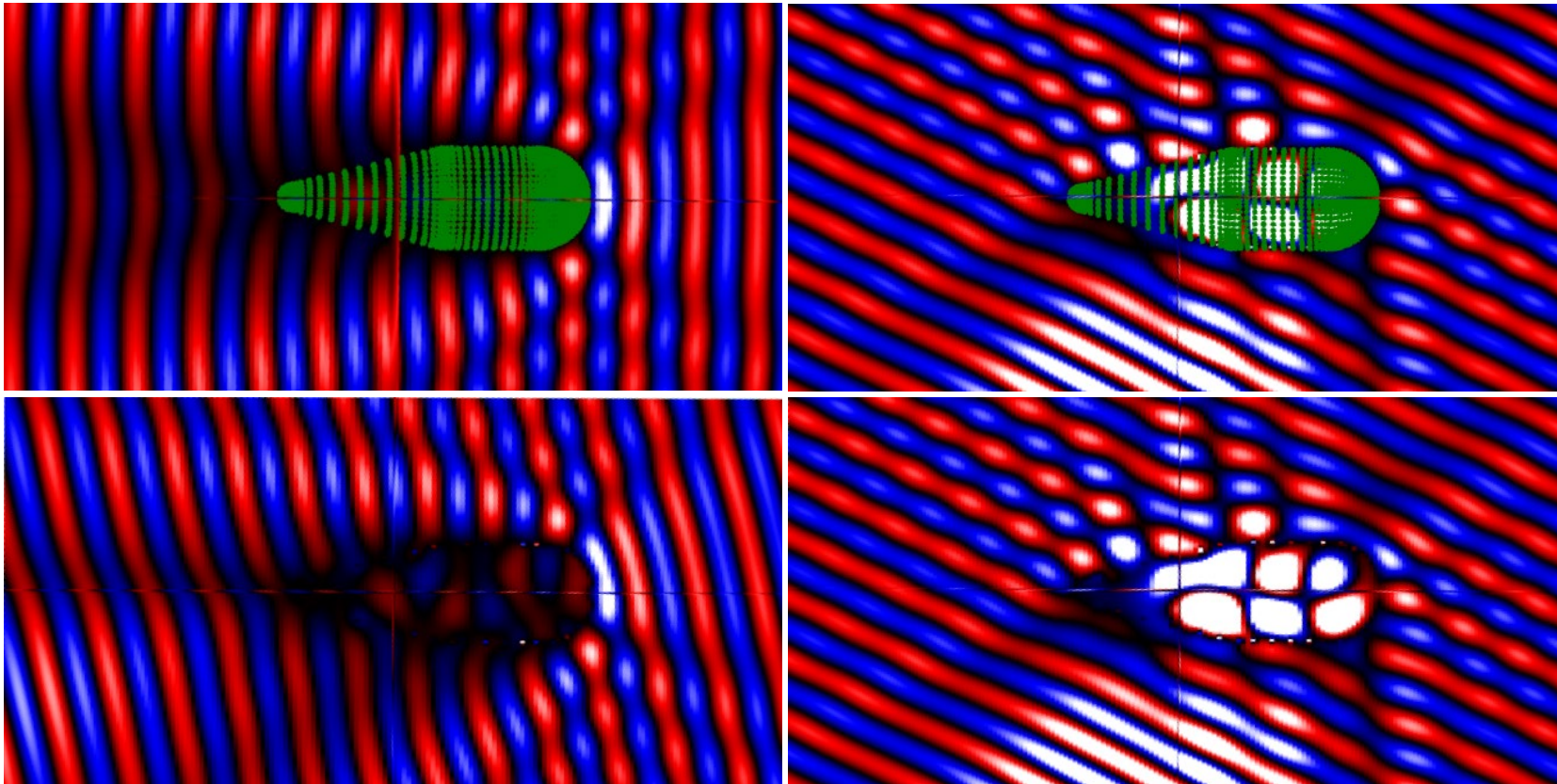
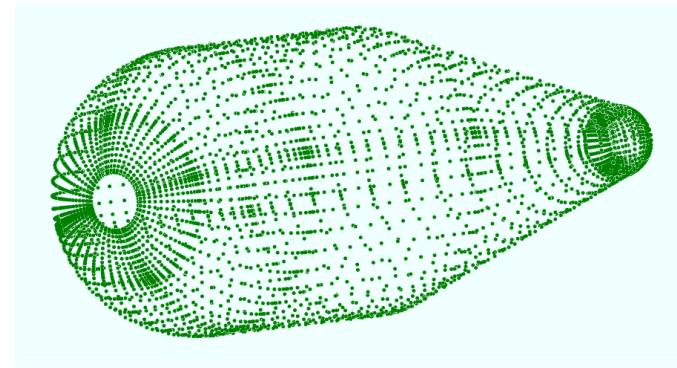




# 3D Cavity Experiments

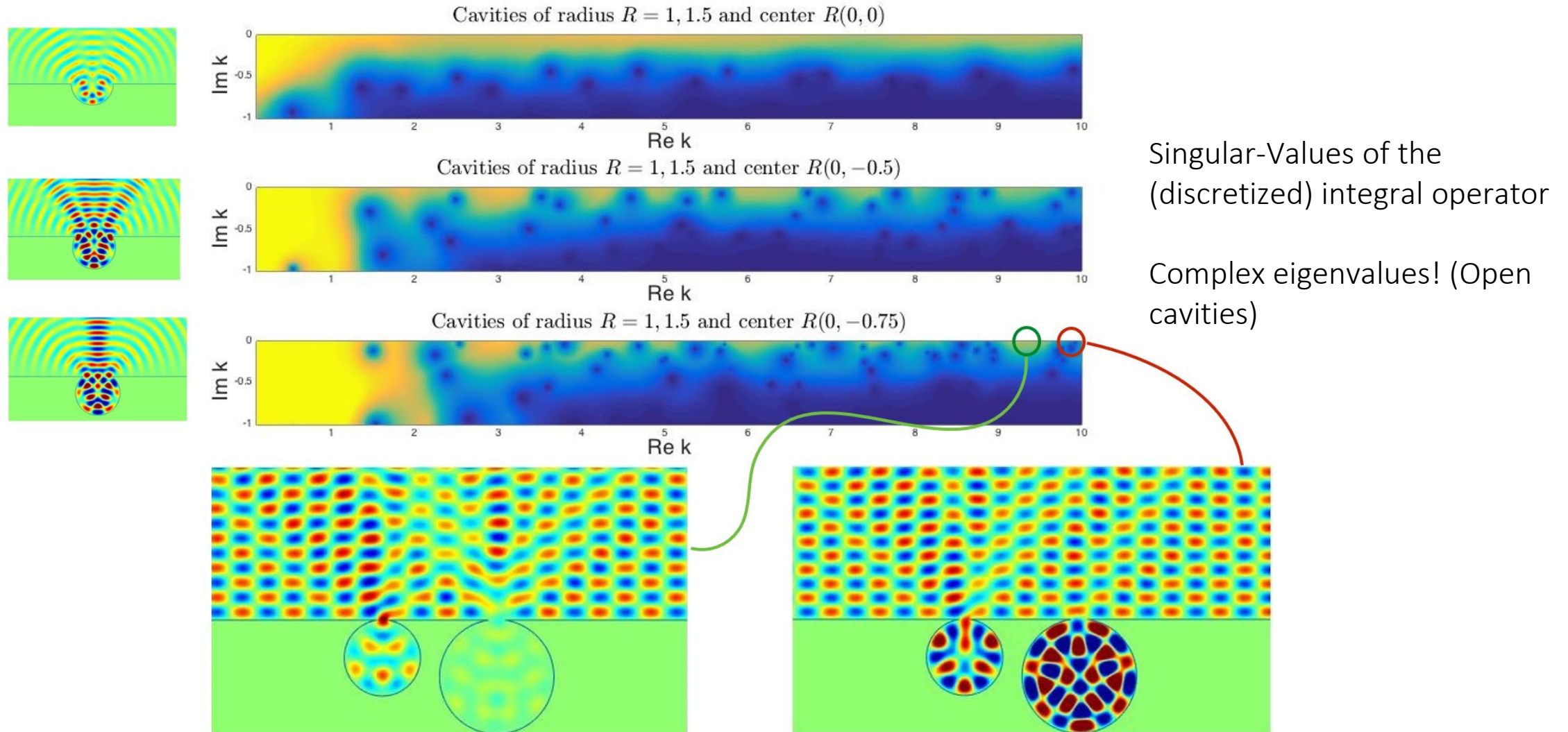
## Resonant Cavity Fields

(Identified by experimentation)



Bruno and Voss [2012] (Unpublished)

# Open Cavity Problems (Frequency domain)



# Frequency-Domain resonances

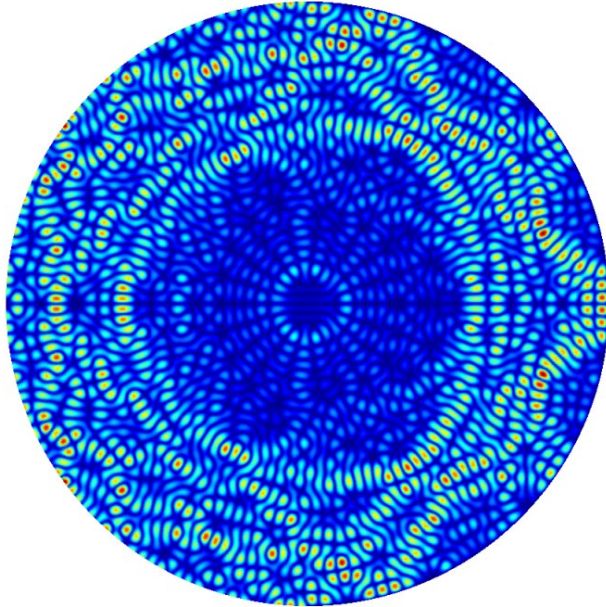
(real and complex eigenvalues)



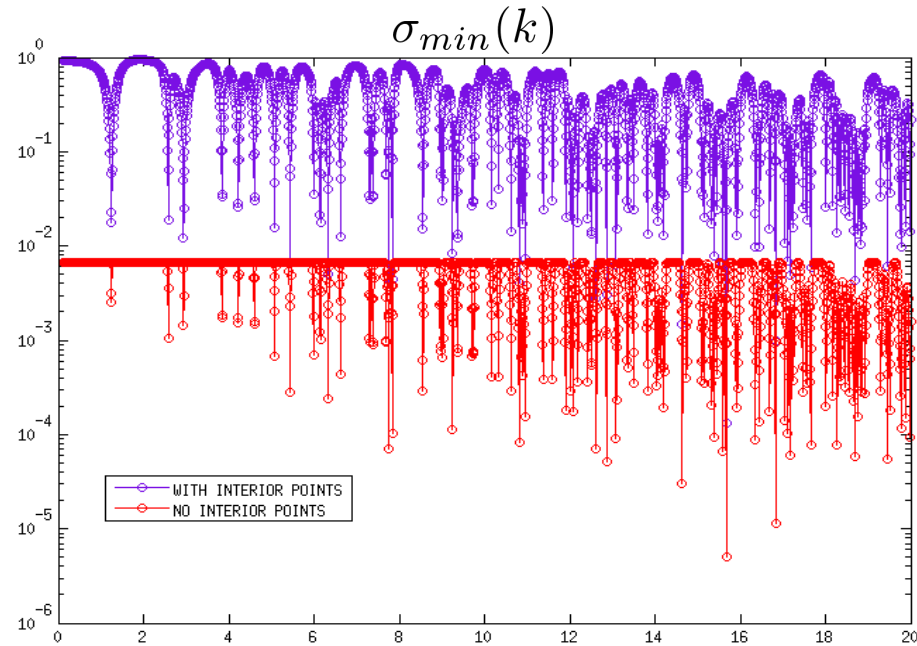
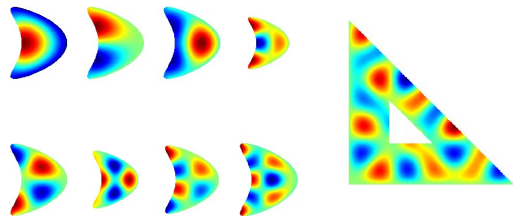
# Integral Eigensolvers

Previous search algorithms: e.g. zero minimum singular value

Mixed: Dirichlet/Neumann



Geometrically flexible!  
(may e.g. use CAD files)



Singular value decomposition at each frequency  
Not viable for high-frequency problems in 3D

Alternatives:

Newton method on determinant  
(Zhao and Barnett [2015], requires  
LU factorization)

Contour integration methods based  
on Cauchy's theorem (Beyn [2012])

New approach:

Scattering solvers on random  
illumination +  
Rational approximants from  
contours (no use of Cauchy's  
theorem)

Akhmetaliyev, Bruno and Nigam, JCP [2015]

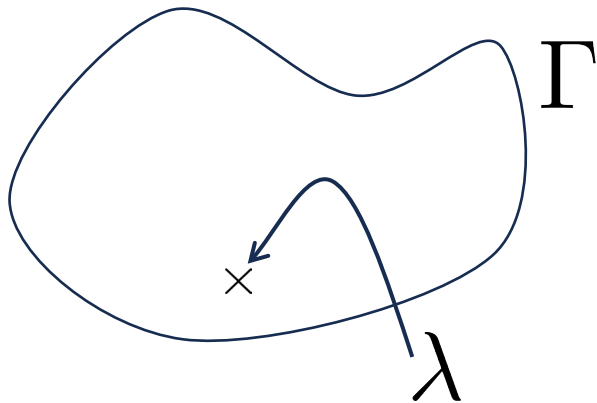


Key Concept in  
Contour Integration Eigensolvers

$$F(z) = c(z - \lambda)$$

$$\frac{1}{2\pi i} \int_{\Gamma} F(z)^{-1} dz = \frac{1}{c}$$

$$\frac{1}{2\pi i} \int_{\Gamma} z F(z)^{-1} dz = \frac{\lambda}{c}$$



For matrix-valued  $F(z)$ ...

$$A_0 = \frac{1}{2\pi i} \int_{\Gamma} F(z)^{-1} R dz = VW^* R,$$

$$A_1 = \frac{1}{2\pi i} \int_{\Gamma} z F(z)^{-1} R dz = VJW^* R$$

# New approach

## (Closed and open cavities)

$$F_k[\psi](x) = \int_{\Gamma} G_k(x, y) \psi(y) ds_y, \quad x \in \Gamma$$

$S(k) = u^T F_k^{-1} v$ , where  $u, v \in \mathbb{C}^n$  are fixed random vectors.

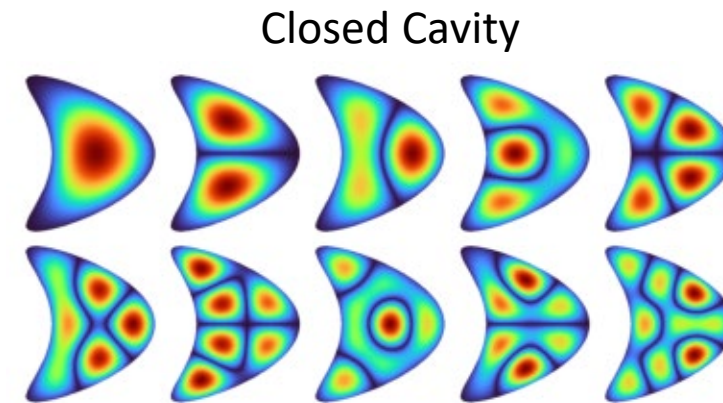
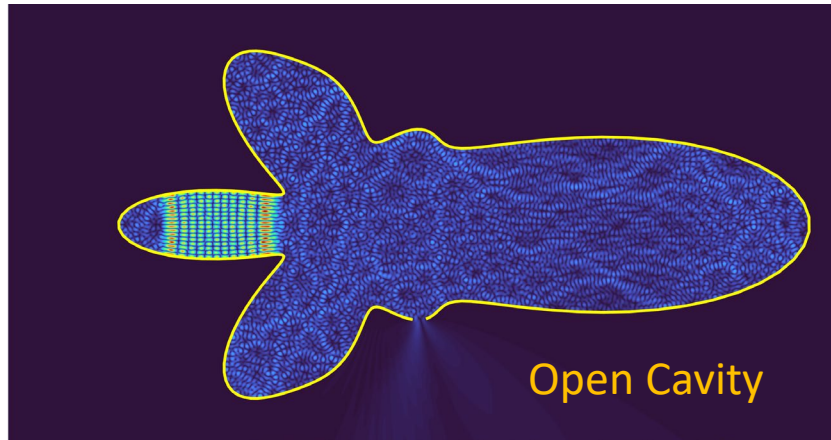
$S(k)$  is a meromorphic function of  $k$

Eigenvalues/scattering poles coincide with the poles of  $S(k)$

AAA rational interpolant of  $S(k)$  ++

$$r(k) = \frac{n^m(k)}{d^m(k)} = \sum_{j=1}^m \frac{w_j^m f_j}{k - k_j} \bigg/ \sum_{j=1}^m \frac{w_j^m}{k - k_j}$$

Their poles closely approximate  
eigenvalues/scattering poles!

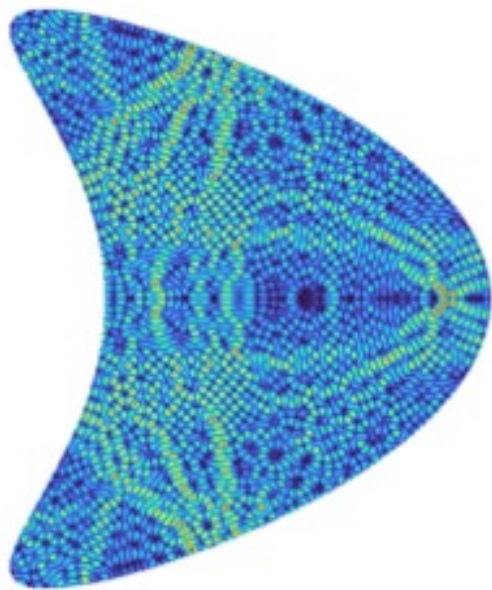


Bruno, Santana and Trefethen  
Submitted [2024] (Available on arXiv)

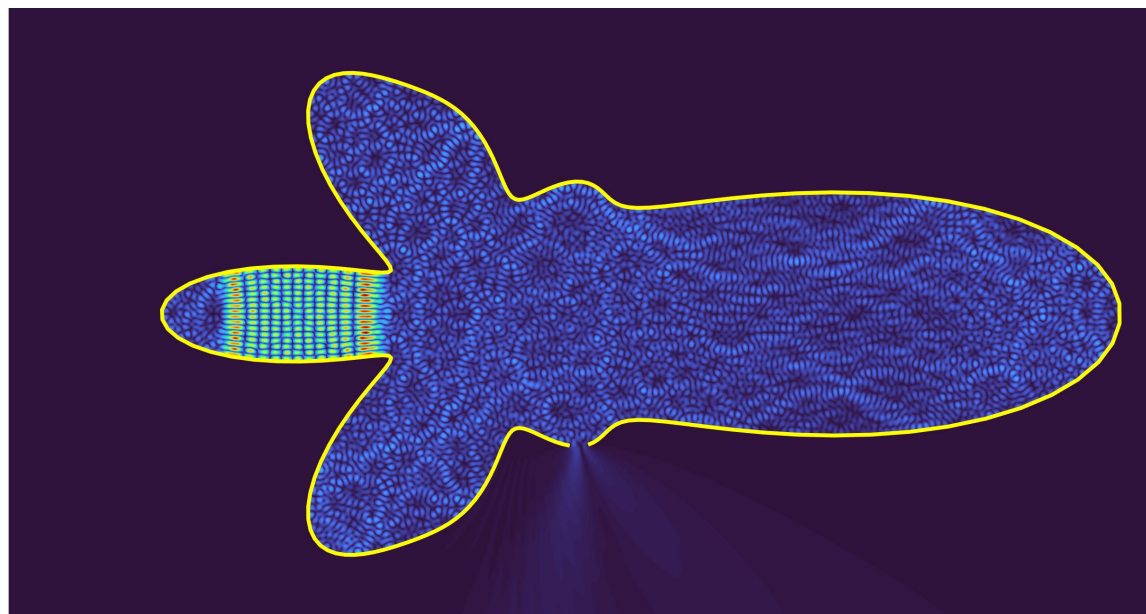
# Resonances

Closed cavities: Real eigenvalues

Open cavities: Complex eigenvalues (also called scattering poles)

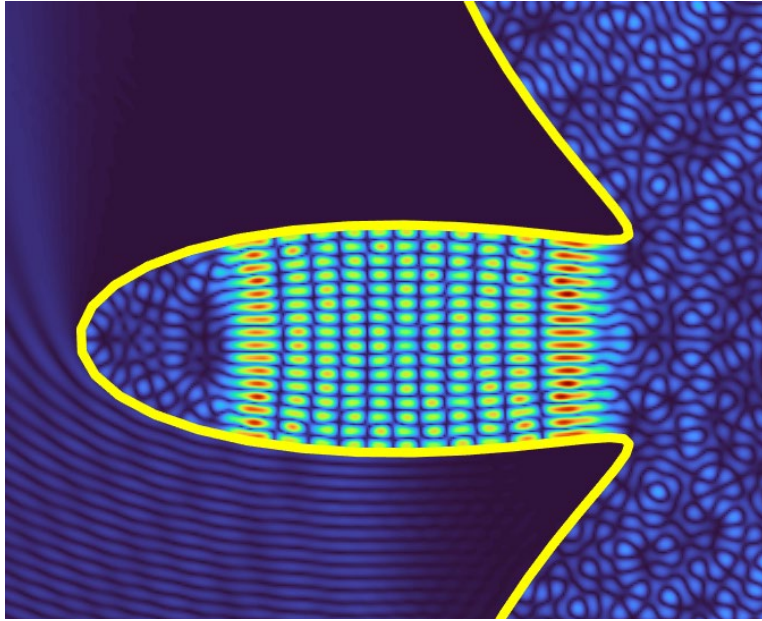


Real eigenvalues

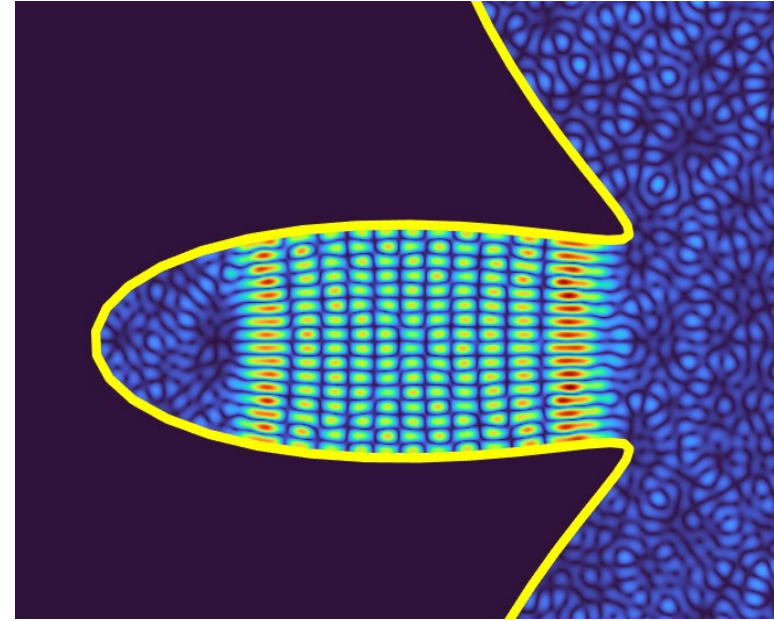


Complex eigenvalues (negative imaginary part)

# Closeup: scattered field vs. eigenfunction



Vertically incident plane  
 $k = 399.9694808817$



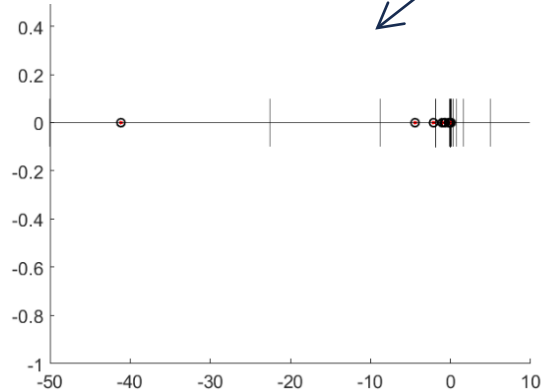
Eigenfunction for the scattering pole at  
 $k = 399.9694808817 - 0.00434495360i$

Up to a small error, a single mode is excited by the incident field!



## "Algorithm 1 with Secant"

- + Rational approximation (via AAA) of  $S(k)$  (matching values along square boundaries)
- + Secant method
- + Adaptivity



## Eigensearch

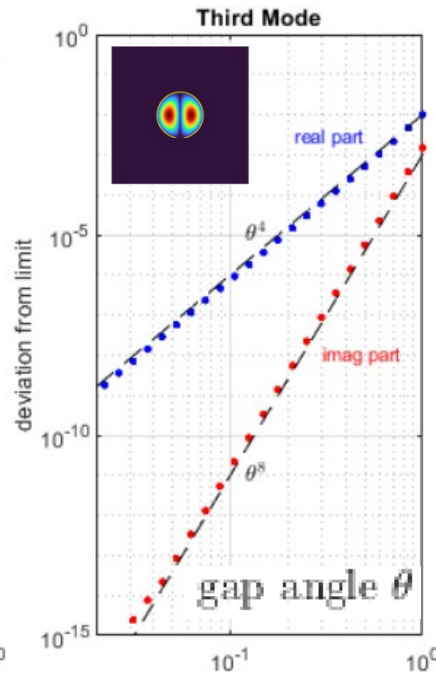
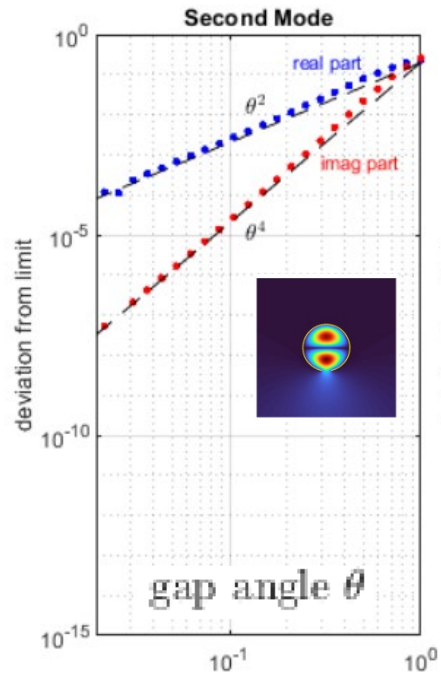
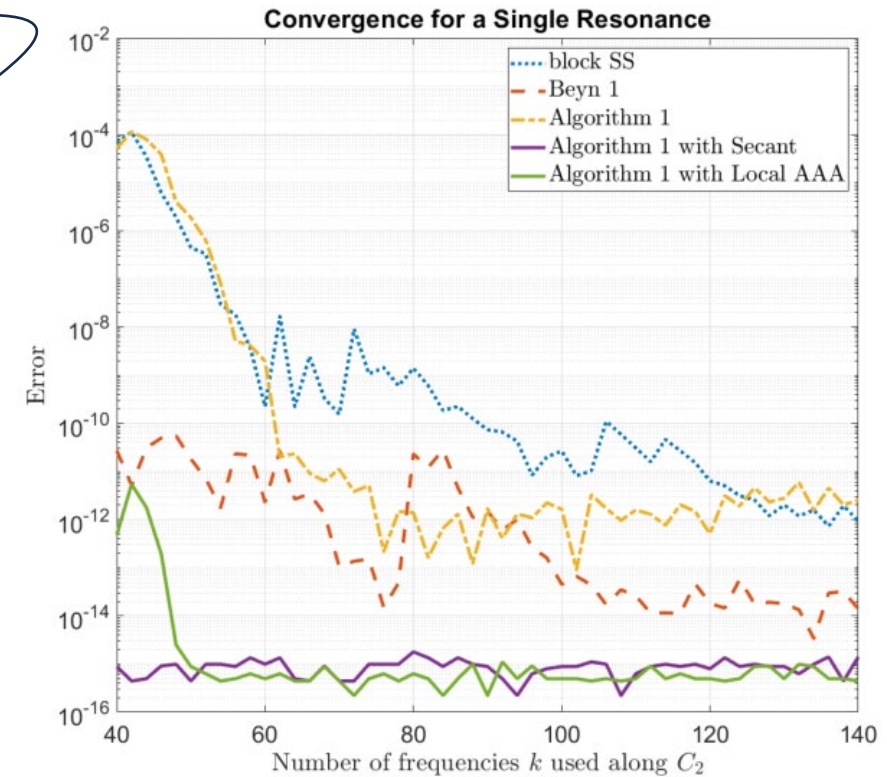
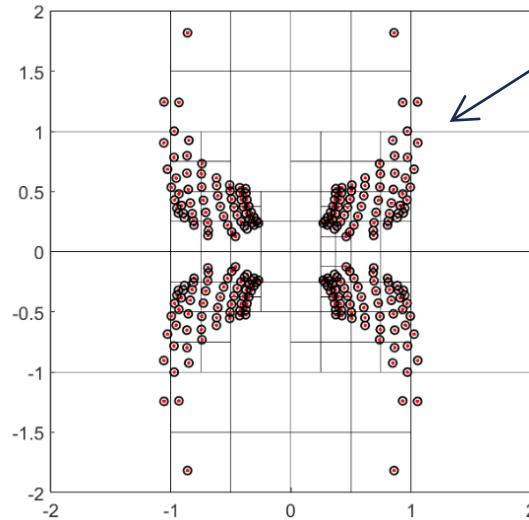
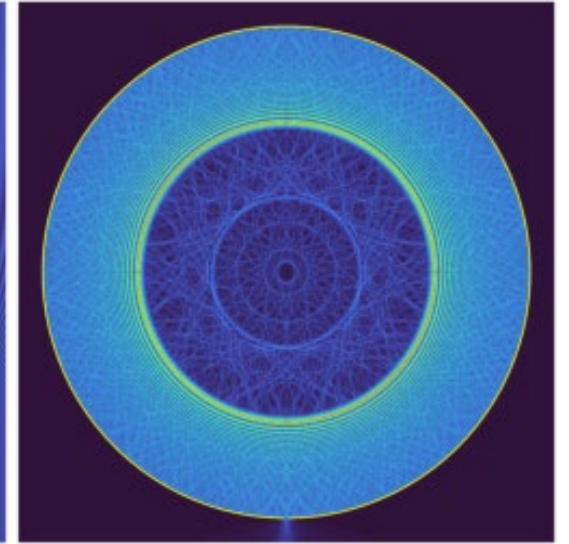
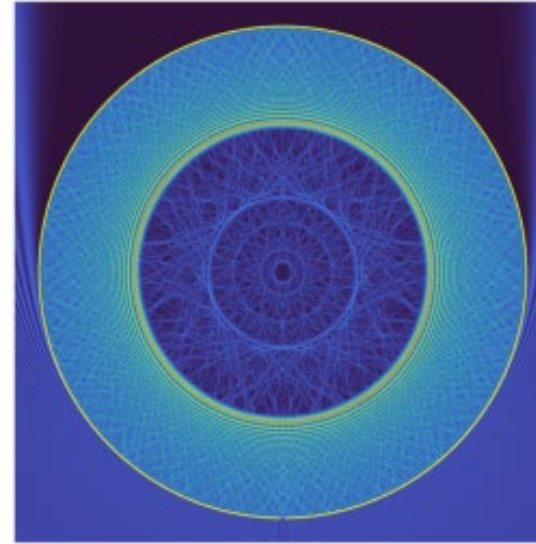
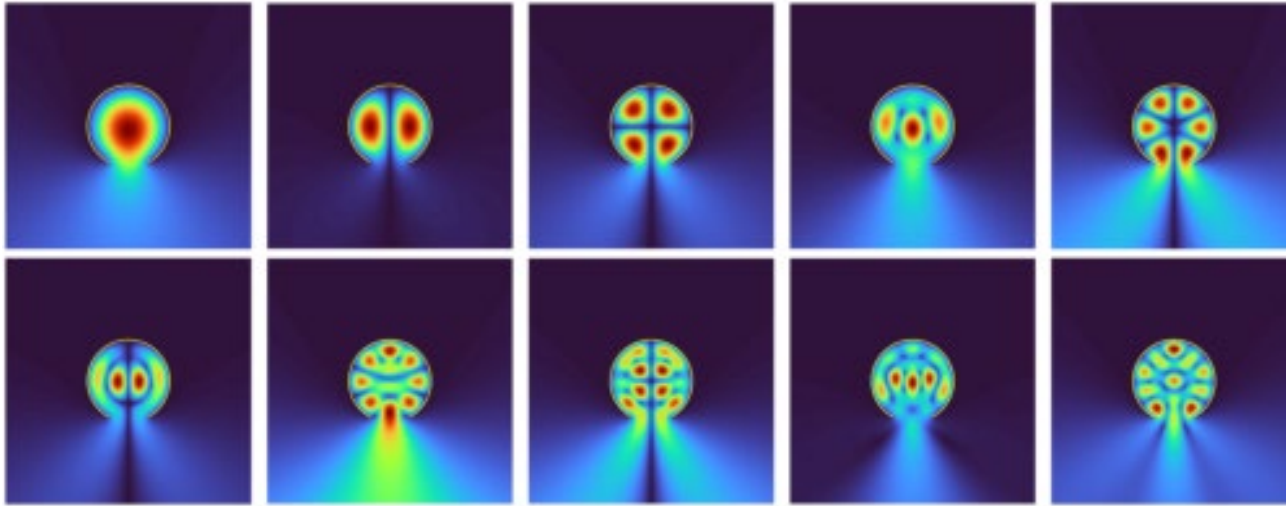


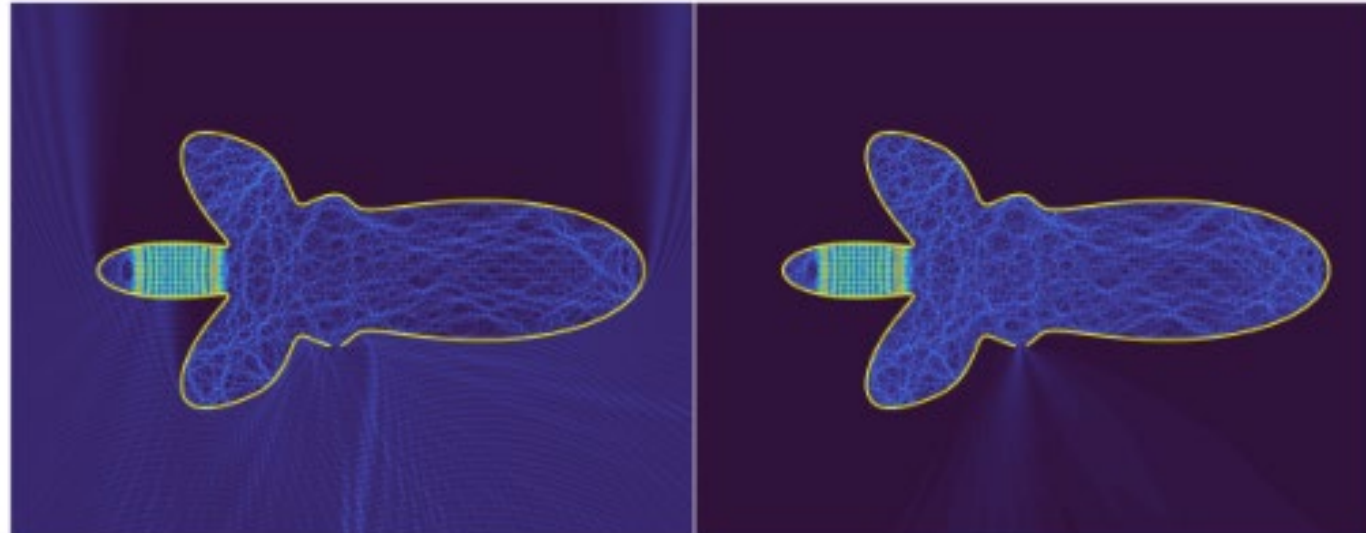
Illustration: Gap closing asymptotics

Bruno, Santana and Trefethen  
Submitted [2024] (Available in arXiv)

# Open Cavities

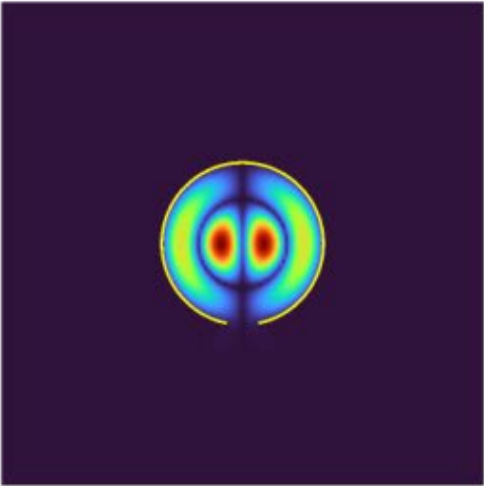
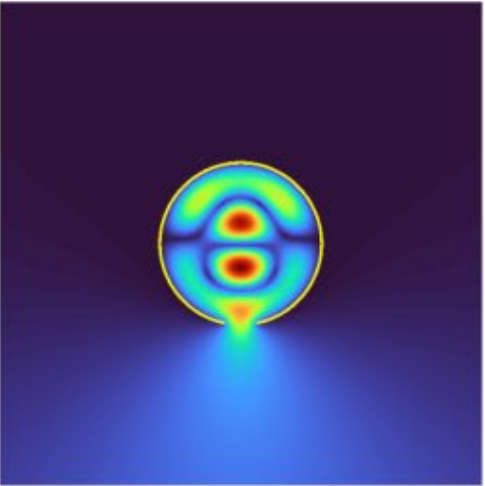
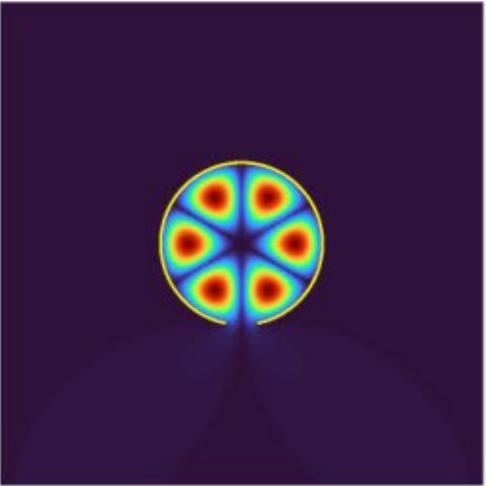
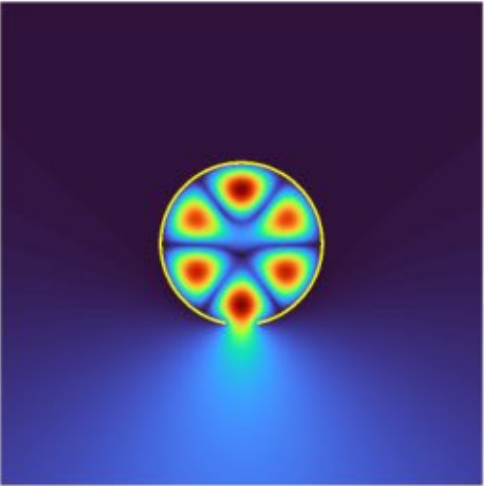
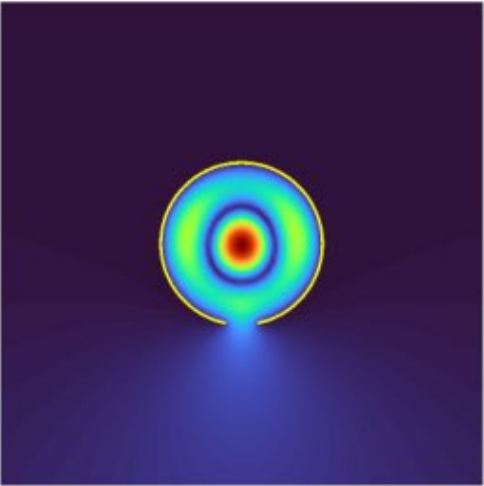
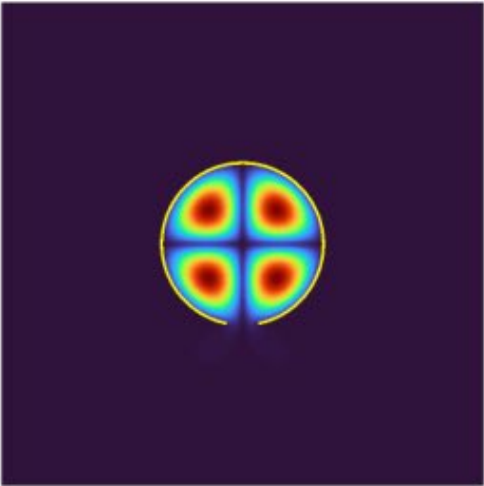
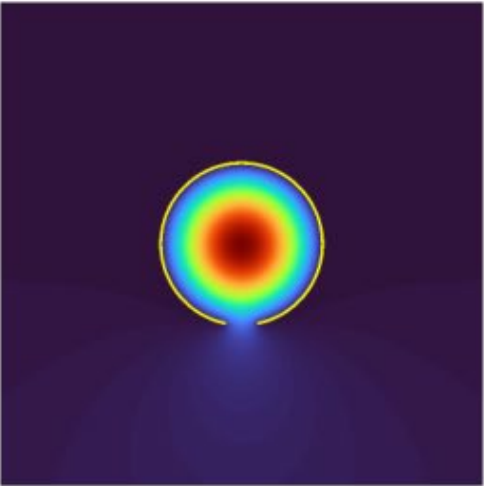


Trial and error scattering frequency  
(Bruno and Lintner, [2012])  
 $k = 400$



Actual scattering pole  
(Bruno, Santana and Trefethen [2024])  
 $k = 399.969480881$

Closed Kite	Open Circle
2.209856180349	2.391850921204 - 0.000866833533i
3.215653682128	3.785851440218 - 0.007551333804i
3.528868275787	3.831519839558 - 0.000000810935i
4.303831479675	5.066410135738 - 0.022753855105i
4.371112240590	5.134599571714 - 0.000011845979i
4.906513621606	5.486798760828 - 0.010839713761i
5.291183742145	6.297659940294 - 0.044691641691i
5.461743432329	6.377232306043 - 0.000071959651i
5.736410337307	6.923647500434 - 0.056416692369i
6.172352448525	7.015195622517 - 0.000013514954i



Slow Time Decay: Singularity Subtraction



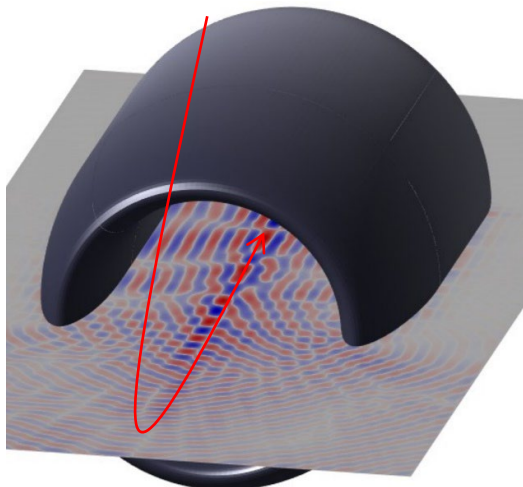
# Time-Decay in Open Cavity Scattering

## Frequency-Time Hybrid Simulation

$$\|A_\omega^{-1}\|_{L^2(\Gamma) \rightarrow L^2(\Gamma)} \leq C(1 + \omega^2)^{q/2}$$

( $A_\omega =$  Integral Operator)

Point Source Pulse

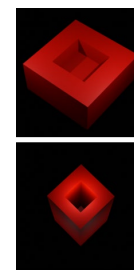


**Theorem (Anderson and Bruno, submitted).** If  $\Gamma$  satisfies the  $q$ -growth condition, then for  $t > T_0$  and for all  $n \in \mathbb{N}$  the integral equation solution  $\psi$  satisfies the time -decay estimate

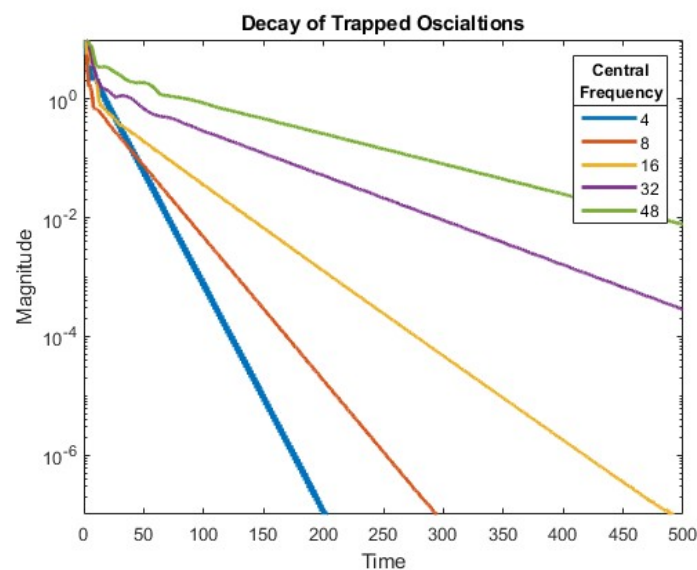
$$\|\psi\|_{H^p([t, \infty); L^2(\Gamma))} \leq C(t - T_0)^{1/2-n} \|\psi\|_{H^{p+(n+1)(q+1)}(I_{T_0}; L^2(\Gamma))}$$

Satisfy the  $q$ -growth condition with  $q = 3$

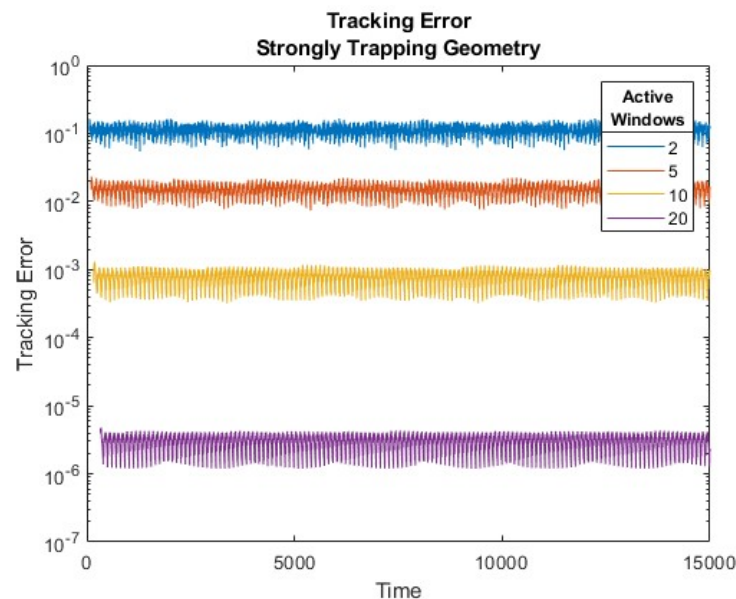
(follows from Chandler-Wilde, Spence, Gibbs, and Smyshlyaev [2020])



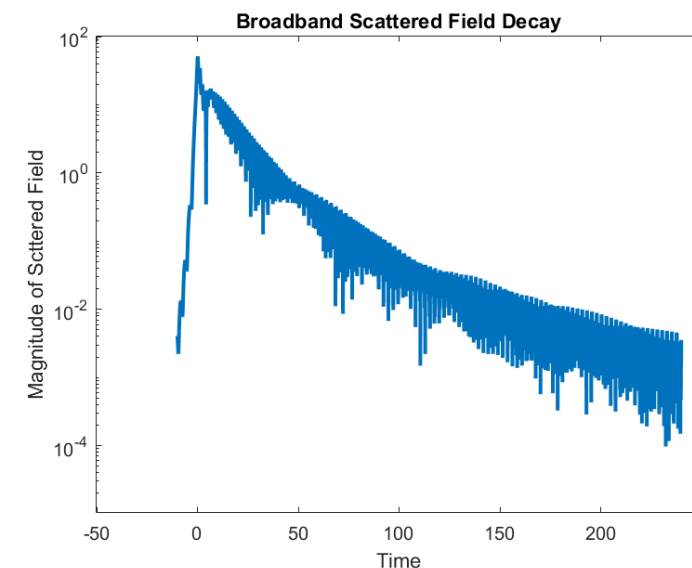
$q = 3$



Frequency-Dependent exponential decay

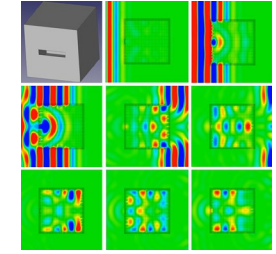


Anderson, Bruno and Lyon (in preparation)

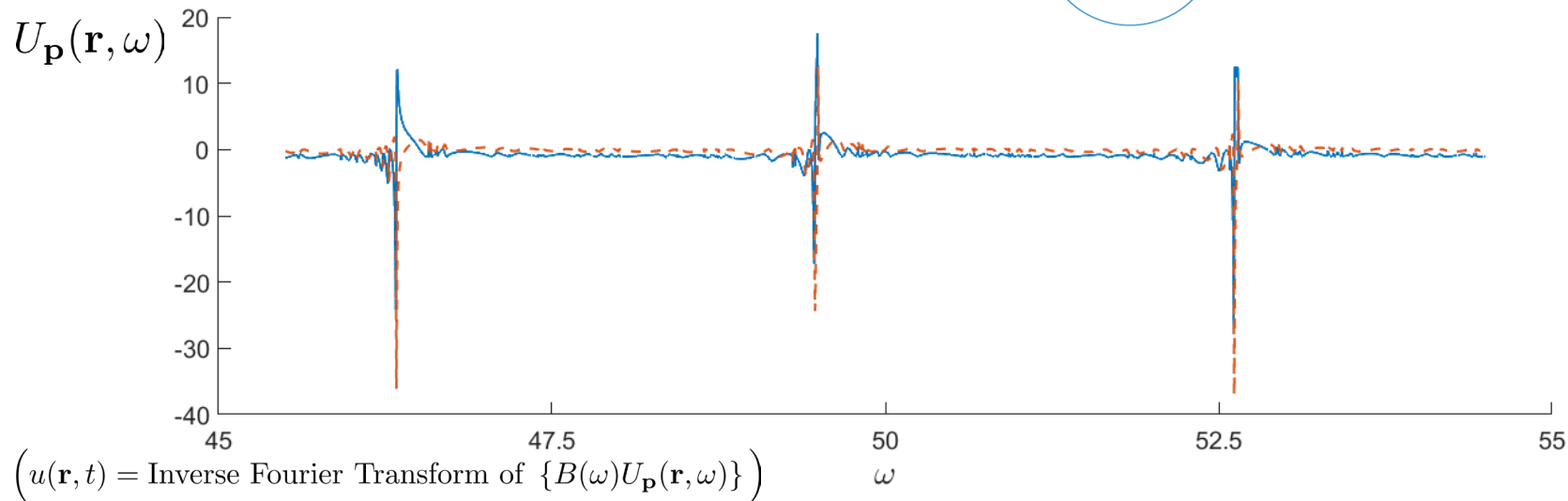
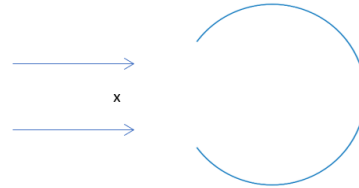


# Frequency-Time Hybrid for Cavity Problems

Eigenvalues (Scattering Poles) close to the real frequency axis induce the main difficulties observed



$$U_{\mathbf{p}}^{\text{inc}}(\mathbf{r}, \omega) = e^{i \frac{\omega}{c} \mathbf{p} \cdot \mathbf{r}} \\ \left( k = \frac{\omega}{c}, \quad c = 1 \right)$$



Eigenvalues (Scattering Poles) close to the real frequency axis

Many frequency-domain solutions are needed to produce sufficiently fine meshes, to allow for the resolution of **pole-induced spikes** at unknown locations

Poles **close to the real axis** induce **slow decay** – and, hence, many cavity temporal cycles

**Frequency-Time Hybrid (FTH)**  
time-domain algorithm:  
an effective time-domain  
wave solver

Open Cavity problems:  
**Accumulation of slowly  
decaying cycles**  
over multiple incidence  
windows (expensive)

Open Cavity problems:  
Require **many frequency-  
domain solutions**  
(expensive)

**Slow decay** —————→

# Singularity Subtraction!

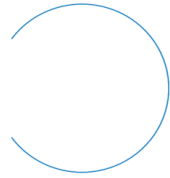
All poles lie in the negative imaginary half-plane

Many Scattering Poles (Eigenvalues) close to the real frequency axis

Illustration

$$U_{\mathbf{p}}^{\text{inc}}(\mathbf{r}, \omega) = e^{i \frac{\omega}{c} \mathbf{p} \cdot \mathbf{r}} \quad \begin{matrix} \longrightarrow \\ x \end{matrix}$$

$(k = \frac{\omega}{c}, \quad c = 1)$



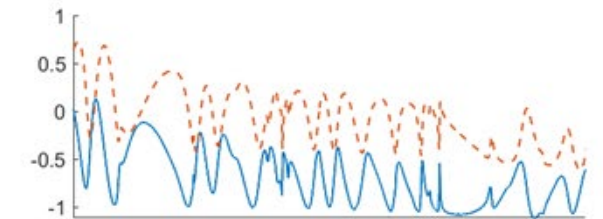
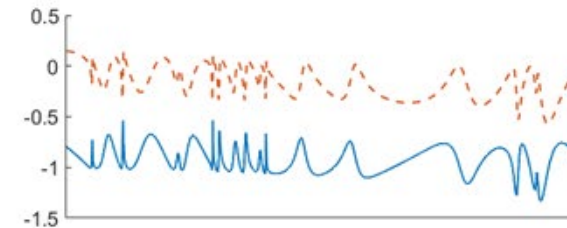
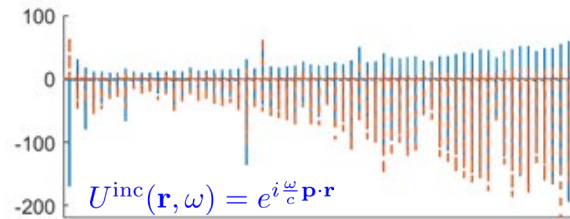
Orange Circles :  $S(k) = u^T F_k^{-1} u^{\text{inc}}$ , where  $v \in \mathbb{C}^n$  is a fixed random vector

Blue Dots :  $S(k) = u^T F_k^{-1} v$ , where  $u, v \in \mathbb{C}^n$  are fixed random vectors

Excited Eigenvalues Only

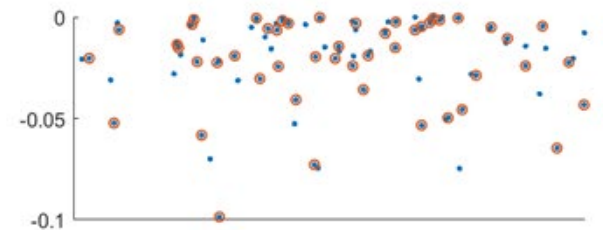
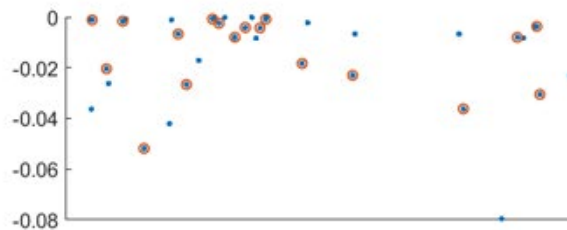
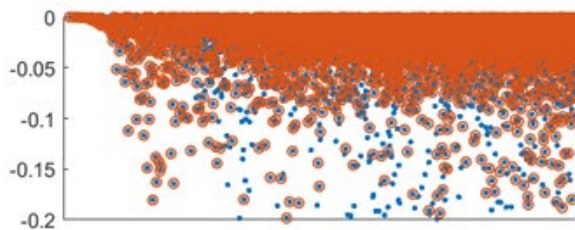
All Eigenvalues

Scattered Field  
at x



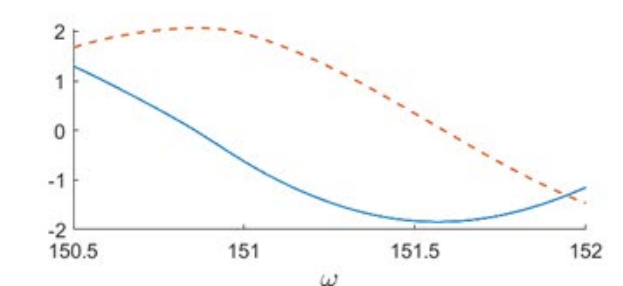
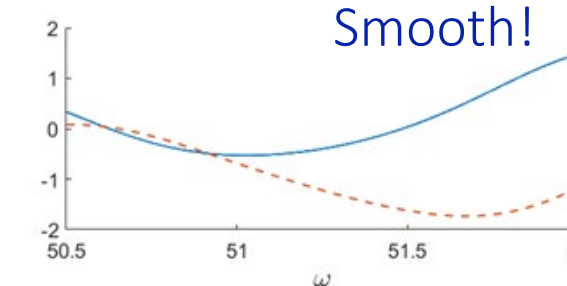
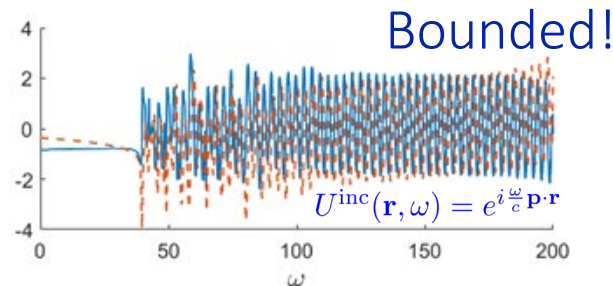
Scattering Poles

Dots: Operator Eigenvalues  
Circles: poles for the  
given incident field



Singularities Subtracted

(Only those circled in orange;  
others are “unimportant”)



# Singularity subtraction

Consider, for example, the time-domain plane wave incident field

Inverse Fourier Transform of  $\{B(\omega)U_{\mathbf{p}}^{\text{inc}}(\mathbf{r}, \omega)\}$   
 (Essentially) Compactly Supported  $\nearrow$  frequency window  $\nwarrow e^{i\frac{\omega}{c}\mathbf{p}\cdot\mathbf{r}}$   
 (Rapidly decaying analytic window function)

Computed at complex  $\omega$  by evaluating AAA rational approximants  
 based on values  $g_{\mathbf{p}}(\mathbf{r}, \omega)$  at real  $\omega$  AAA support points

$U(\mathbf{r}, \omega) = B(\omega)g_{\mathbf{p}}(\mathbf{r}, \omega)$  where  $g_{\mathbf{p}}(\mathbf{r}, \omega) = \int_{\Gamma} G_{\omega}(\mathbf{r}, \mathbf{r}')\psi_{\mathbf{p}}(\mathbf{r}', \omega)d\sigma(\mathbf{r}')$ .

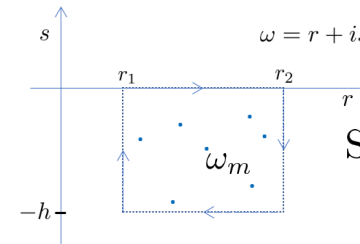
Integral equation solution for boundary values  $U_{\mathbf{p}}^{\text{inc}}$

$u(\mathbf{r}, t) = \frac{1}{2\pi} \int_{-\infty}^{\infty} U(\mathbf{r}, \omega)e^{-i\omega t}d\omega$

Residue:  $c_m(\mathbf{r}) = \frac{1}{2\pi i} \int_C g_{\mathbf{p}}(\mathbf{r}, \omega)d\omega$

Singularity Subtraction smoothed density:

$$g_{\mathbf{p}, \text{smth}}^h(\mathbf{r}, \omega) = g_{\mathbf{p}}(\mathbf{r}, \omega) - \sum_{m=1}^{M_h} \frac{c_m(\mathbf{r})}{\omega - \omega_m}$$



Simple poles assumed, for simplicity

$u(\mathbf{r}, t) = \frac{1}{2\pi} \int_{-\infty}^{\infty} B(\omega)g_{\mathbf{p}, \text{smth}}^h(\mathbf{r}, \omega)e^{-i\omega t}d\omega + \frac{1}{2\pi} \sum_{m=1}^{M_h} c_m(\mathbf{r}) \int_{-\infty}^{\infty} \frac{B(\omega)}{\omega - \omega_m} e^{-i\omega t}d\omega$

$\sim -2\pi i B(\omega_m)e^{-i\omega_m t}$   
 ↑  
 Decaying oscillatory exponential

$\nwarrow \sim 0$



# Singularity subtraction vs. Singularity Expansion

The asymptotic expansion

$$u(\mathbf{r}, t) \sim -i \sum_{m=1}^{M_h} c_m(\mathbf{r}) B(\omega_m) e^{-i\omega_m t}$$

that is a byproduct of the previous calculation is known in the literature as a...

- “Singularity Expansion” (SE), after Lax and Phillips [1962], Baum [1970] and others
- A focus in the literature has been to determine the validity of the approximation of  $u(\mathbf{r}, t)$  by the SE
- The Lax-Phillips theory establishes exponential asymptotic approximation as  $t \rightarrow \infty$  *for non-trapping obstacles only*
- The Singularity Subtraction (SS) method does not require asymptotic approximation from the SE term. The SS method is valid even at times for which SE does not accurately represent the field  $u(\mathbf{r}, t)$
- Indeed, the SS method merely subtracts the sum of polar singularities to eliminate the spikes from the frequency domain data, and then it adds back the contribution from the SE—whether correct or incorrect
- In particular, the SS is rigorously valid for arbitrary obstacles, including highly-trapping obstacles
- As it happens, however, the SS formalism provides a strong indication that formulation provides correct asymptotic approximation for arbitrary scatterers, including trapping obstacles

# Background on SEM

Zworski 2000 indicates that

For nontrapping obstacles Lax and Phillips [1967/1989] established that

$$\left. \begin{aligned} (\partial_t^2 - \Delta) u(t, x) &= 0, \quad x \in \mathbb{R}^n \setminus \mathcal{O}, \\ u|_{t=0} &= f \in \mathcal{C}_c^\infty(\mathbb{R}^n \setminus \overline{\mathcal{O}}) \\ \frac{1}{i} \partial_t u|_{t=0} &= g \in \mathcal{C}_c^\infty(\mathbb{R}^n \setminus \overline{\mathcal{O}}) \end{aligned} \right\} \Rightarrow \quad (1)$$
$$u(t, x) = \sum_{\operatorname{Im} \lambda_l \leq C} \sum_{j=1}^{m_{\mathcal{O}}(\lambda_l)} w_{\lambda_l, j}(x) e^{it\lambda_l} t^{j-1} + \mathcal{O}\left(e^{-(C-\varepsilon)t}\right), \quad x \in \mathbb{R}^3 \setminus \mathcal{O},$$

where  $m_{\mathcal{O}}(\lambda_l)$  is the multiplicity of the resonance ( $\operatorname{Im} \lambda_l \geq 0$  convention).

---

Baum [1976] writes

The general SEM formalism began [in 1971] [from experimental observations concerning the transient electromagnetic response of complicated scatterers such as missiles and aircraft](#). It was observed that [damped sinusoids](#) were dominant features of typical transient responses. Such damped sinusoids corresponded to [pole pairs in the \[s-plane\]](#).

Poles were one type of singularity in the s plane and [this led to the concept of using all the s plane singularities to form a description of the transient and frequency-domain responses](#). It was also noted that the poles corresponded to the natural frequencies which had been discussed in some of the older literature (Stratton [1941]).

# Transients and asymptotics. General domains!

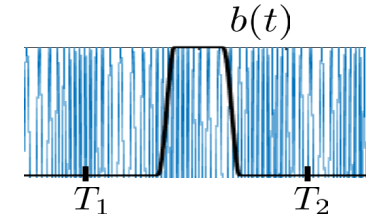
(Arbitrary trapping character. Windowed time signal in a given frequency band.)

$$\omega = r + is, \quad s < 0$$

$$B(\mathbf{r}, \omega) = \int_{T_1}^{T_2} b(\mathbf{r}, t) e^{irt - st} dt = \underbrace{e^{-sT_2}}_{\text{Large}} C(\mathbf{r}, \omega), \quad \text{where}$$

$$C(\mathbf{r}, \omega) = \int_{T_1}^{T_2} b(\mathbf{r}, t) e^{irt + s(T_2 - t)} dt$$

Bounded for all  $s < 0$   
 $\approx 0$  for  $r \leq r_1$  and  $r \geq r_2$  (some  $r_1$  and  $r_2$ ),  $s < 0$



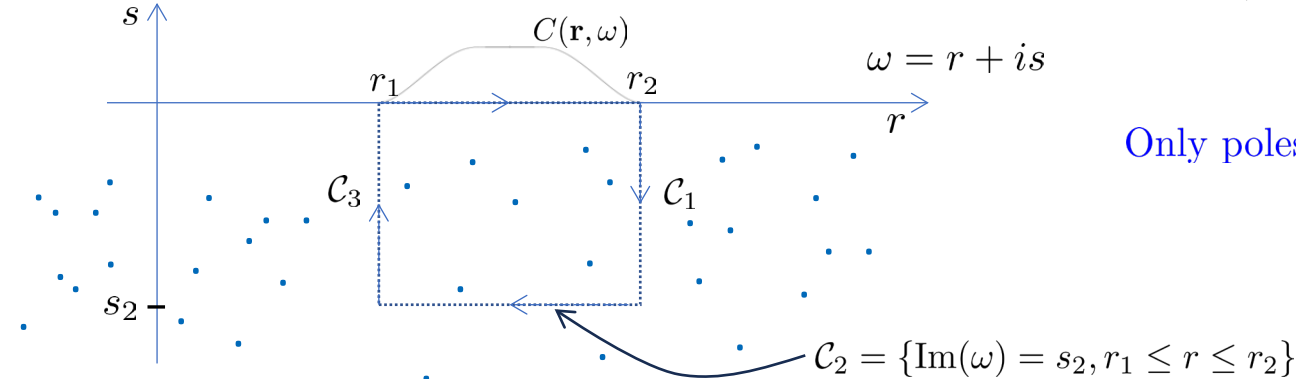
$$u(\mathbf{r}, t) = \frac{1}{2\pi} \int_{r_1}^{r_2} e^{-i\omega t} d\omega \underbrace{\int_{\Gamma} G_{\omega}(\mathbf{r}, \mathbf{r}') \psi_B(\mathbf{r}', \omega) d\sigma(\mathbf{r}')}_{U_C(\mathbf{r}, \omega)} \quad (s = 0)$$

$$U(\mathbf{r}, \omega) = e^{-sT_2} U_C(\mathbf{r}, \omega) \quad (s \leq 0)$$

$$U_C(\mathbf{r}, \omega) = \int_{\Gamma} G_w(\mathbf{r}, \mathbf{r}') \psi_C(\mathbf{r}', \omega) d\sigma(\mathbf{r}')$$

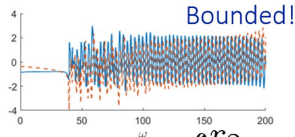
Cauchy's Theorem and Residues

applied to  $U(\mathbf{r}, \omega)$



Only poles within the contour  
are included

Singularities Subtracted  
(Only those circled in orange;  
others are "unimportant")



$r_1$  and  $r_2$  are picked so that the vertical segment contributions are less than a prescribed error tolerance; e.g. machine precision (cf. "Boundedness" images in previous viewgraph for SS fields, and consider that the incident field is windowed)

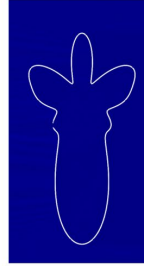
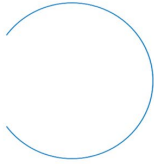
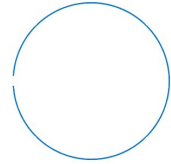
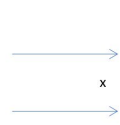
$$\int_{C_2} U(\mathbf{r}, \omega) e^{-i\omega t} d\omega = \int_{r_1}^{r_2} d\omega e^{-i\omega t} e^{-sT_2} \int_{\Gamma} G_w(\mathbf{r}, \mathbf{r}') \psi_C(\mathbf{r}', \omega) d\sigma(\mathbf{r}') = \underbrace{e^{s(t-T_2)}}_{\text{Exponentially small for } t > T_2} \int_{r_1}^{r_2} e^{-irt} dr \int_{\Gamma} G_w(\mathbf{r}, \mathbf{r}') \psi_C(\mathbf{r}', \omega) d\sigma(\mathbf{r}')$$

Exponentially small for  $t > T_2$   
Faster than all enclosed residues

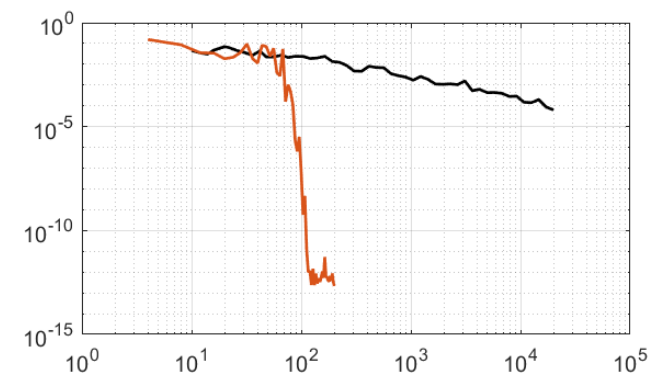
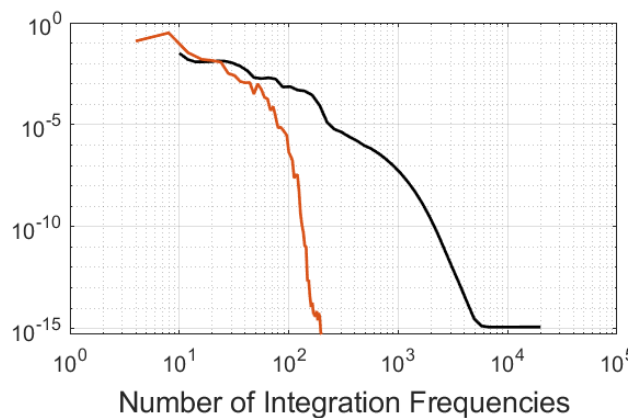
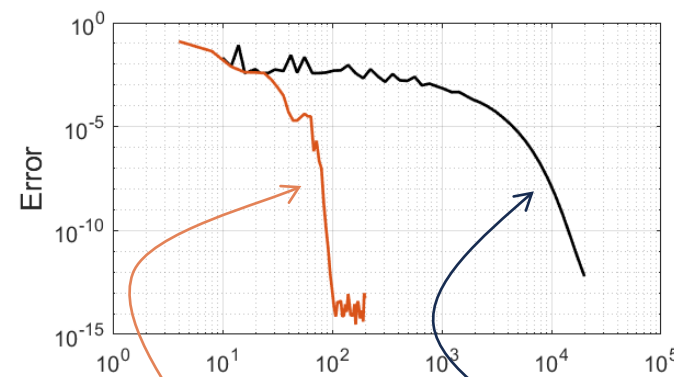
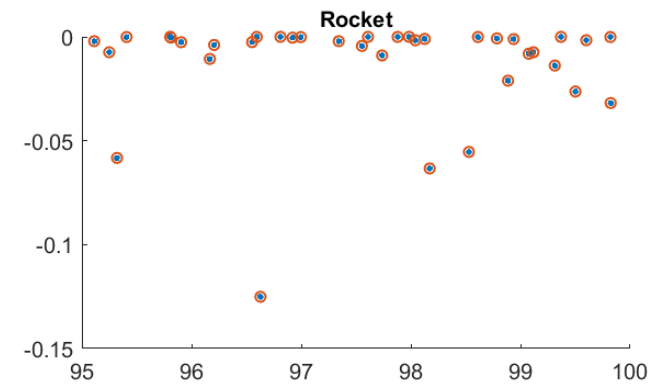
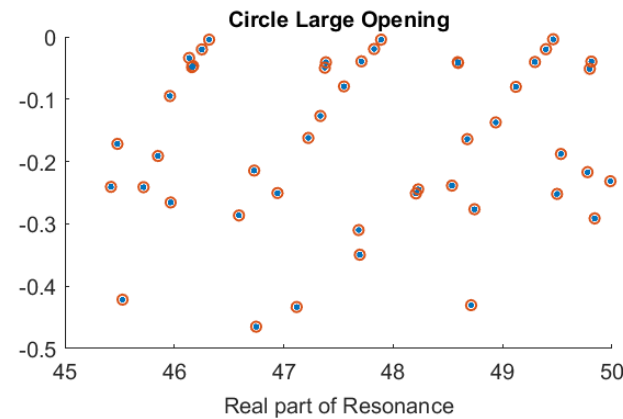
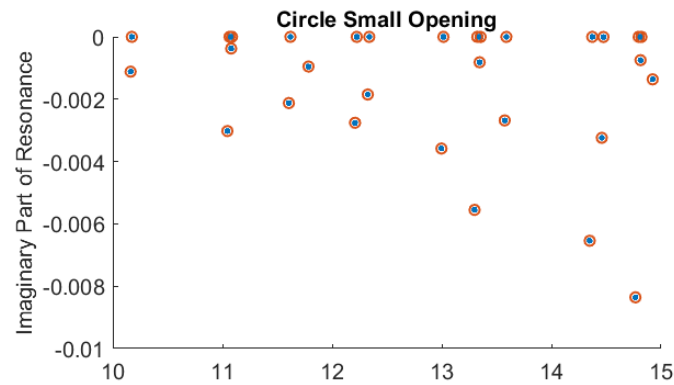
# Singularity Subtraction

$$u^{\text{inc}}(x, t) = e^{ikx - i\omega t}$$

$$\left(k = \frac{\omega}{c}, \quad c = 1\right)$$



Eigenvalue Frequency Solutions  
Re-Used for Time-Field Evaluation!

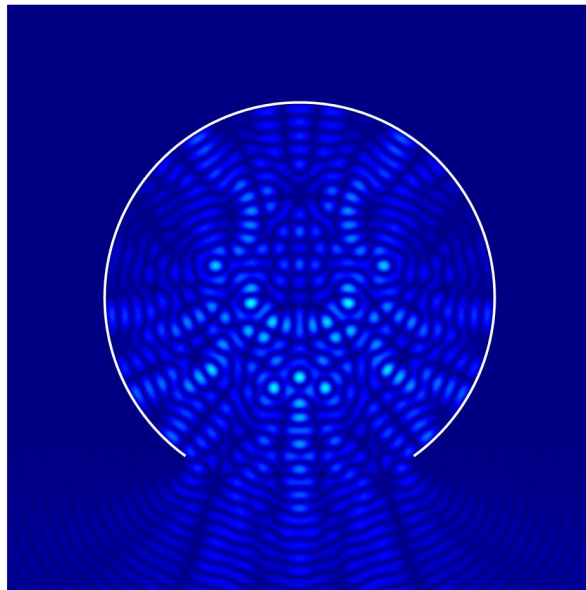
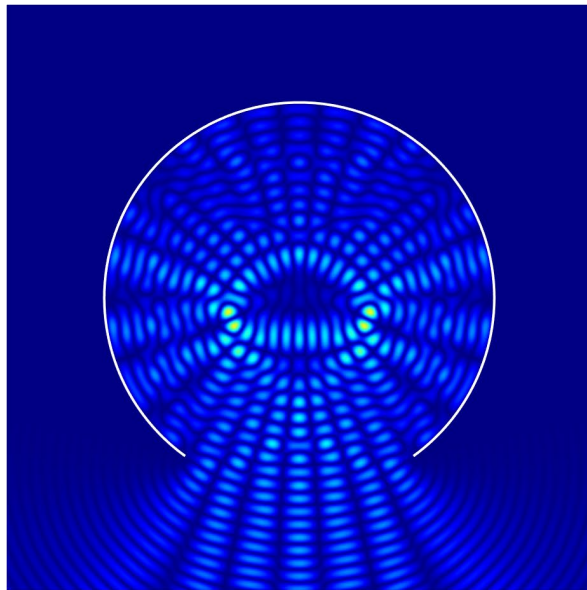
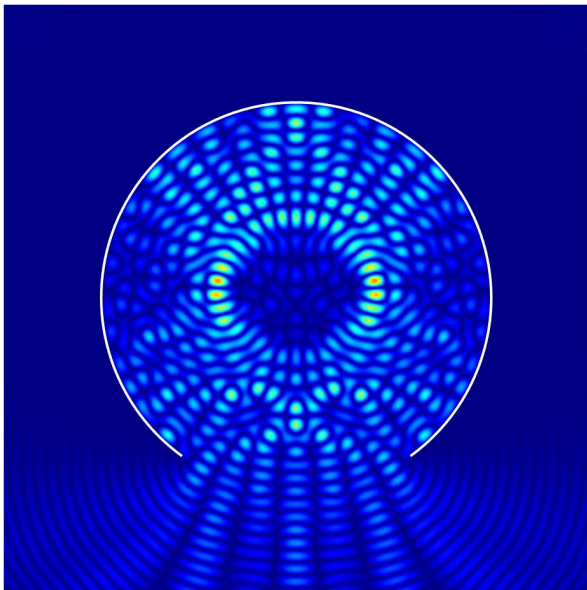
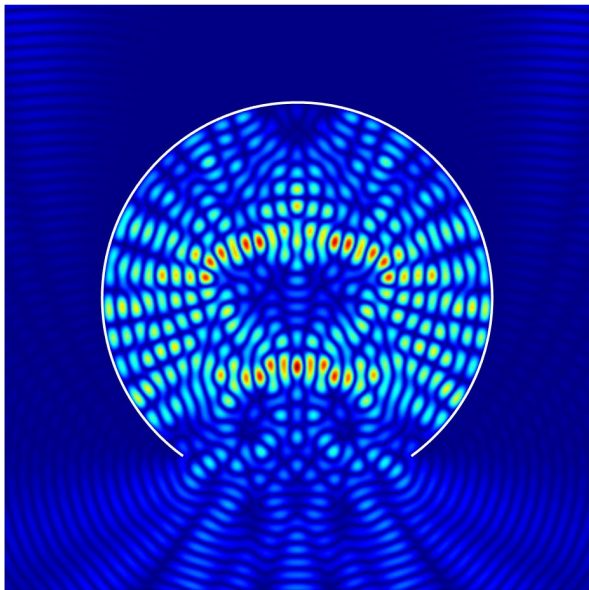
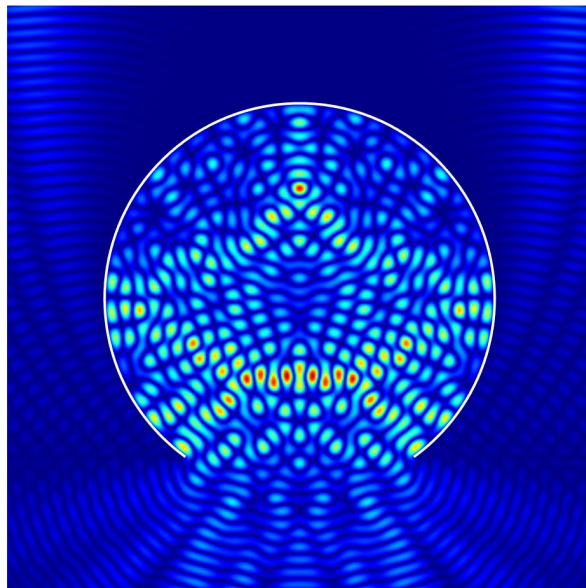
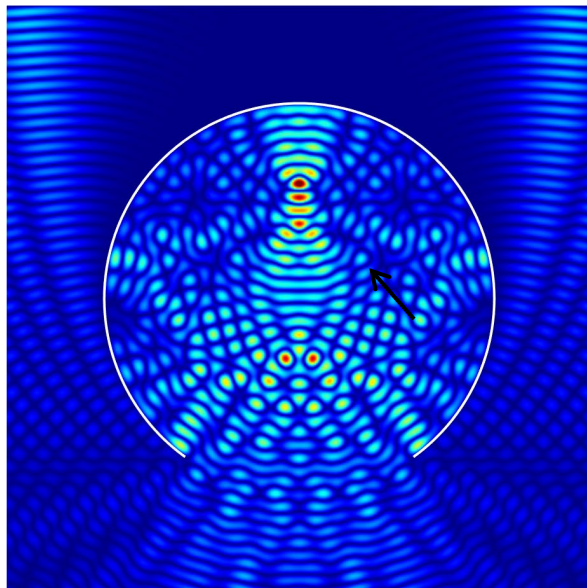
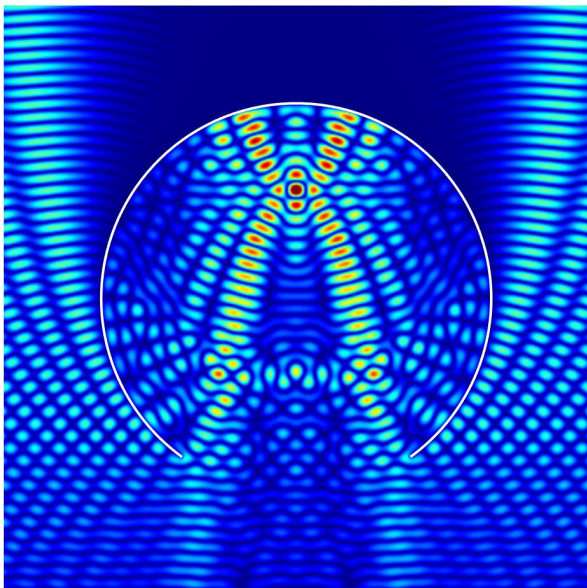
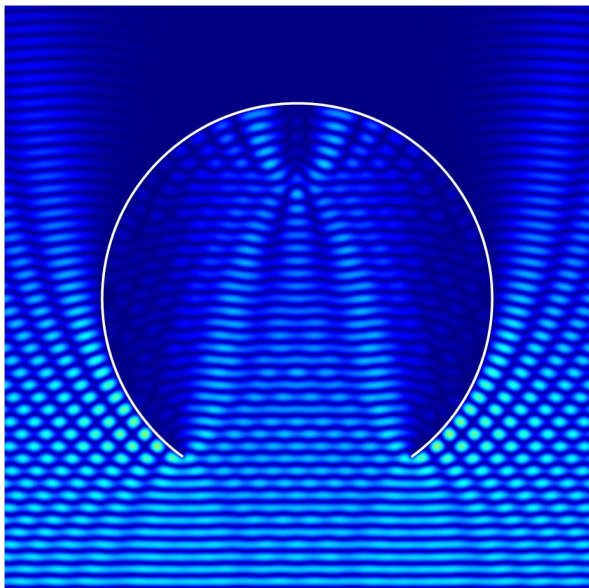


Singularity Subtraction

No Singularity Subtraction

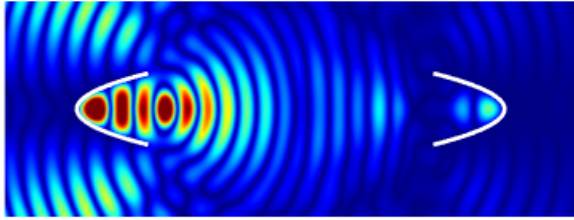
O. Bruno and M. Santana, in preparation [2024]



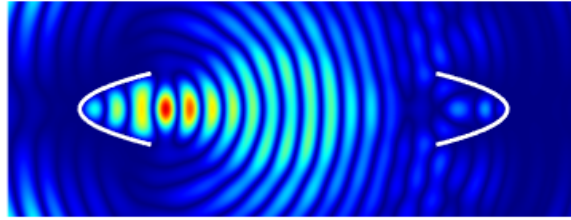


# Whispering Gallery via Singularity Subtraction

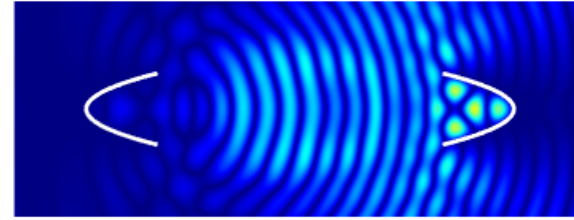
$t = 59.7$



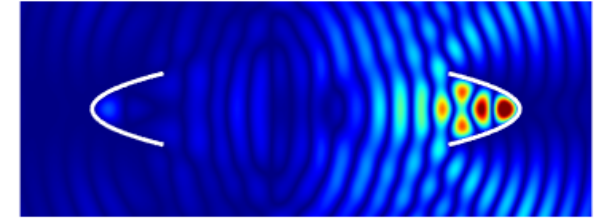
$t = 62.5$



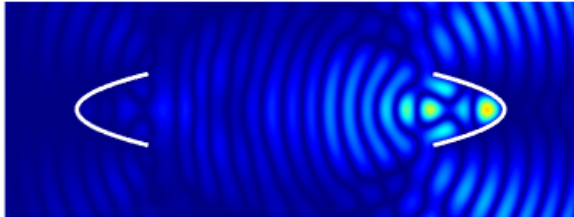
$t = 65.7$



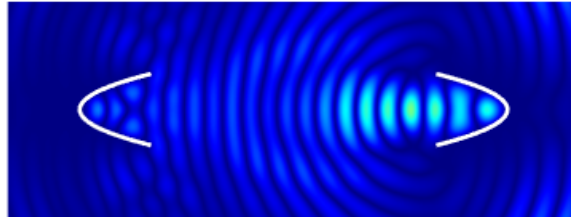
$t = 68.5$



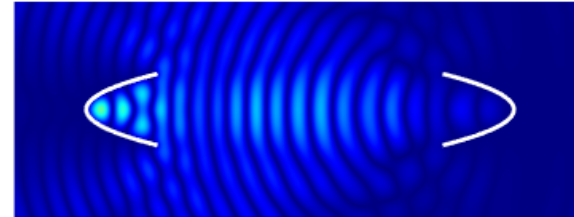
$t = 71.7$



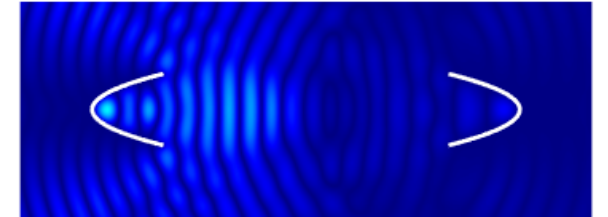
$t = 74.5$



$t = 77.8$



$t = 80.6$

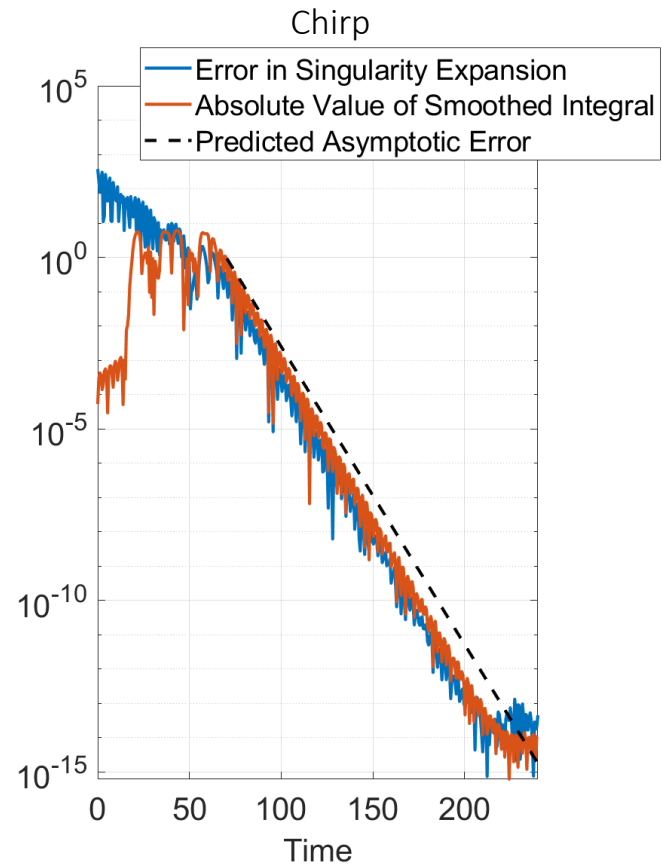
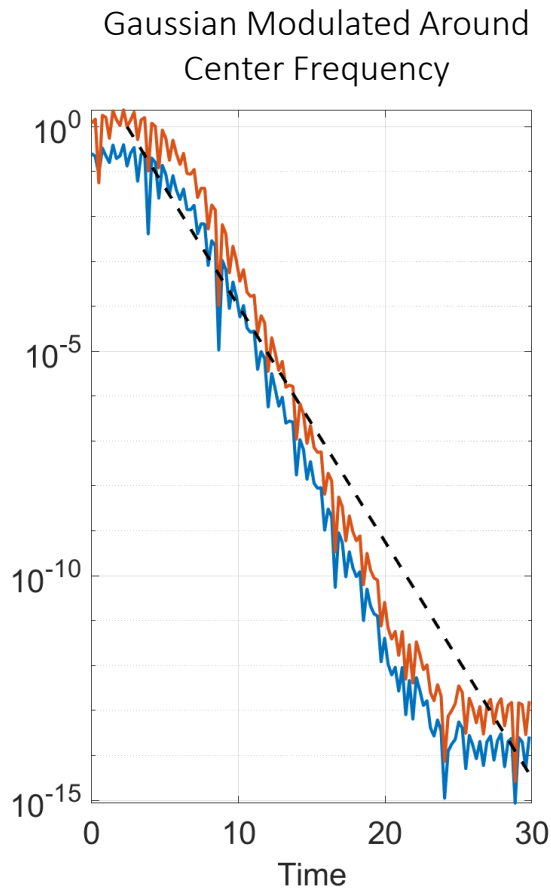
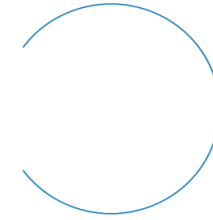




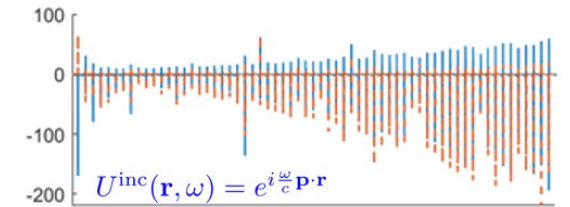
# Error in Singularity Expansion

$$u^{\text{inc}}(x, t) = e^{ikx - i\omega t}$$

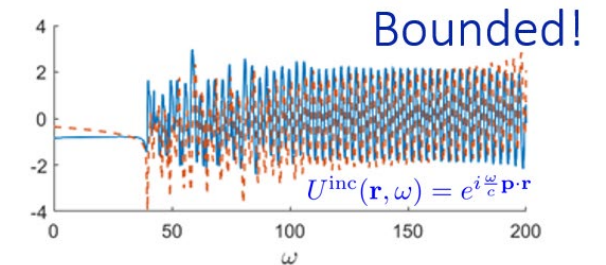
$$\left(k = \frac{\omega}{c}, \quad c = 1\right)$$



Scattered Field  
at  $x$



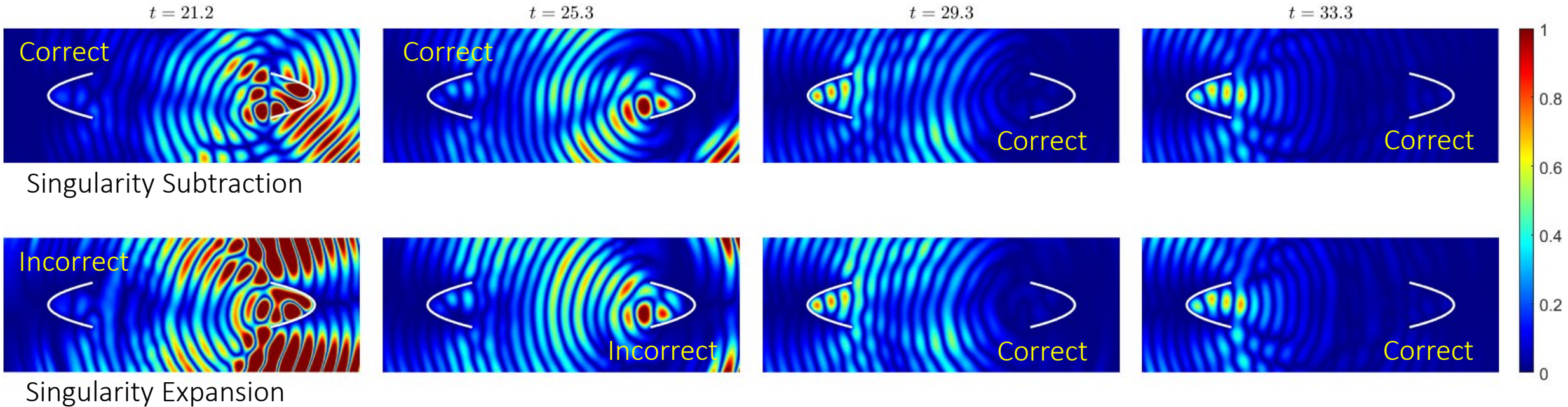
Singularities Subtracted  
(Only those circled in orange;  
others are “unimportant”)



# Singularity Subtraction vs. Singularity Expansion

Scattered field  $u^{\text{scat}}(\mathbf{r}, t)$

$$(u^{\text{tot}}(\mathbf{r}, t) = u^{\text{inc}}(\mathbf{r}, t) + u^{\text{scat}}(\mathbf{r}, t))$$





# Application to Target Identification

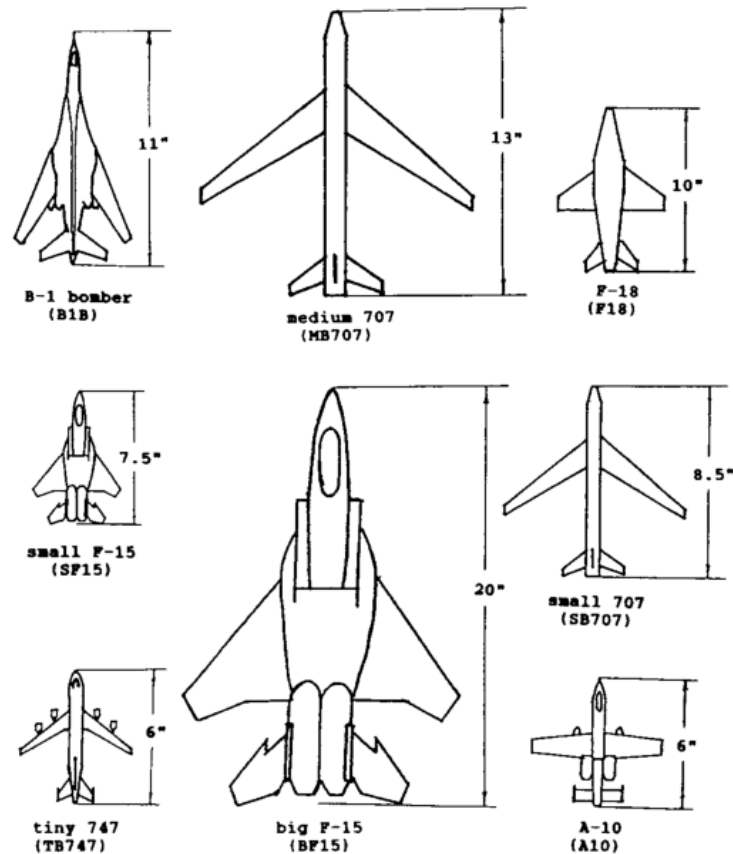


**Fig. 2.** Eight target models used in discrimination experiments in the free-field chamber scattering range.

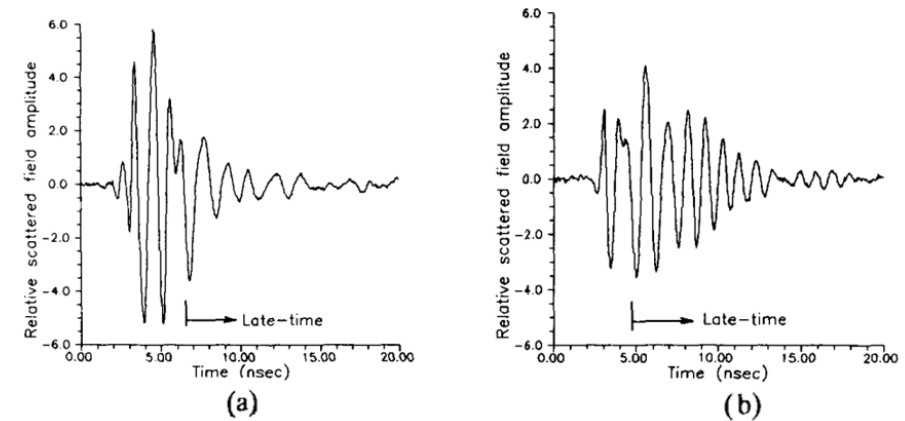


**Fig. 3.** Scattered field pulse responses of (a) big F-15 and (b) A-10 target models measured at 45° aspect.

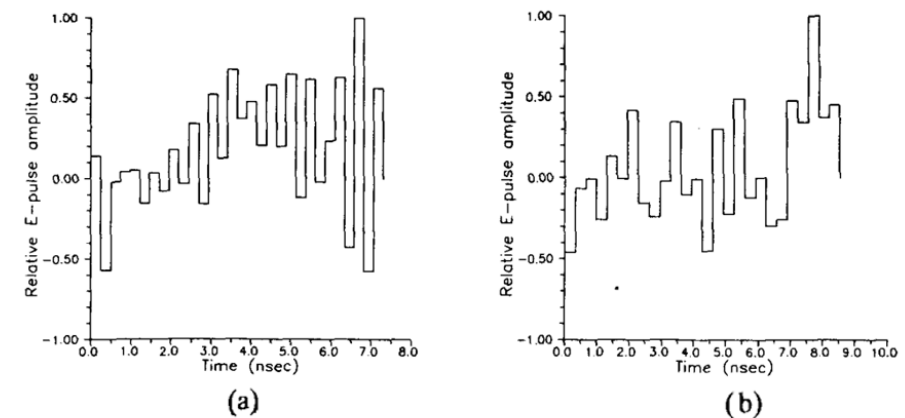
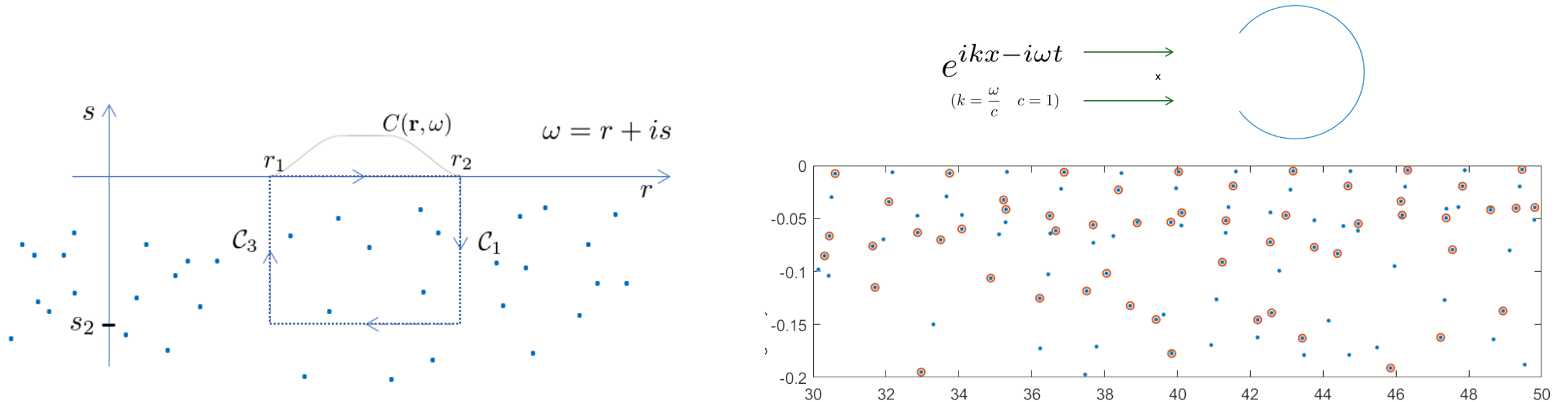


**Fig. 4.** E-pulses constructed to eliminate the modes of the (a) big F-15 and (b) A-10.

# Application to Target Identification



- Only the poles directly below the real “frequency band” are excited. This can be used single out pole structures that are characteristic of one object but not present other objects, under all possible illuminations.
- Could utilize this concept to design incident fields that are closely tuned to a particular class of obstacle, and by varying obstacle orientation, and focusing on just a few poles at a time
- Pole patterns should characterize the corresponding target obstacles
- Pole pattern obtained from backscattered fields by means of the AAA rational approximation algorithm
- Objects could then be identified from their pole patterns by means of an adequate Neural Network classification algorithm

# Resonances and Singularity Subtraction: Summary

- Frequency-domain resonances evaluated as poles of rational approximants with adaptivity and a secant method termination stage
- All-time time-domain scattered field seamlessly captured by a combination of a Singularity Expansion (SE) and a smoothed Singularity Subtracted (SS) Fourier integral
- No requirement of validity of the SE
- However, the asymptotic validity of the SE even for trapping obstacles is suggested by the methods theoretical basis and associated numerical illustrations
- Applications to target identification suggested

